

Multi-scale sequence correlations increase proteome structural disorder and promiscuity

Ariel Afek and David B. Lukatsky*

Department of Chemistry, Ben-Gurion University of the Negev, Beer-Sheva 84105 Israel

*Corresponding Author

Email: lukatsky@bgu.ac.il

Phone: +972-86428370

Fax: +972-86472943

Abstract

Numerous experiments demonstrate a high level of promiscuity and structural disorder in organismal proteomes. Here we ask the question what makes a protein promiscuous and structurally disordered. We predict that multi-scale correlations of amino acid positions within protein sequences statistically enhance the propensity for promiscuous intra- and inter-protein binding. We show that sequence correlations between amino acids of the same type are statistically enhanced in structurally disordered proteins and in hubs of organismal proteomes. We also show that structurally disordered proteins possess a significantly higher degree of sequence order than structurally ordered proteins. We develop an analytical theory for this effect and predict the robustness of our conclusions with respect to the amino acid composition and the form of the microscopic potential between the interacting sequences. Our findings have implications for understanding molecular mechanisms of protein aggregation diseases induced by the extension of sequence repeats.

Introduction

Understanding molecular mechanisms providing specificity of protein-protein binding within a cell has been challenged by recent experimental evidences that the majority of proteins in higher eukaryotes are either entirely or partially intrinsically disordered and thus each such protein poses an ensemble of structures [1]. Numerous experimental evidences suggest that proteins within a cell maintain a high degree of non-specificity [2,3]. Such non-specific binding is termed protein ‘promiscuity’. Organismal-scale measurements of protein-protein interactions (PPI) demonstrate that the entire organismal proteomes possess a high degree of multi-specificity [4,5,6,7,8], with many proteins (‘hubs’) physically interacting with tens and even hundreds of partners. It is predicted that hub proteins possess a higher level of intrinsic disorder as compared with non-hub proteins [9,10]. A key question is what makes a protein promiscuous? Are there generic sequence signatures of promiscuity? In this paper we predict that protein sequences with the enhanced correlations of sequence positions of amino acids of the same type generally represent more structurally disordered and more promiscuous sequences. In particular, we show that sequences of structurally disordered proteins possess significantly stronger correlations than sequences of structurally ordered proteins, such as all-alpha and all-beta proteins. We also show a strong signature of the predicted effect in hub proteins of eukaryotic organisms.

Intuitively, sequence ‘correlations’ mean statistically significant repeats of sequence patterns. The existence of periodicities in protein sequences has been known since the seminar works of Eisenberg *et al* [11,12,13,14,15,16]. Most of these investigations show that sequence periodicities arise due to the existence of symmetrical structural elements such as alpha helixes and beta sheets. More recently sequence periodicities have been also observed in disordered proteins [17,18,19,20,21]. Here we suggest a mechanism that explains why and predicts which sequence correlations induce structural disorder and enhance promiscuity.

Results

We first analyze the non-redundant dataset of structurally disordered proteins [22] (Materials and Methods). The comparison of sequence correlation properties of structurally disordered proteins with all-alpha proteins shows that disordered proteins are significantly stronger correlated than perfectly structured proteins. We characterize the correlation properties of amino acid positions within protein sequences by the normalized correlation function,

$$\eta_{\alpha\beta}(x) = g_{\alpha\beta}(x) / \langle g_{\alpha\beta}^r(x) \rangle, \quad \text{Eq. (1)}$$

where $g_{\alpha\beta}(x)$ is the probability to find a residue of type α separated by the distance x from a residue of type β , and $\langle g_{\alpha\beta}^r(x) \rangle$ is the corresponding probability for the randomized sequence averaged with respect to different random realizations (see Materials and methods). If $\eta_{\alpha\beta}(x) > 1$, then the two residues α and β are statistically correlated at the distance x ; while for entirely random sequences, $\eta_{\alpha\beta}(x) = 1$. The twenty diagonal elements, $\eta_{\alpha\alpha}(x)$, of the entire correlation matrix, $\eta_{\alpha\beta}(x)$, for both disordered and all-alpha proteins datasets are represented in Figure 1. The comparison of disordered proteins with all-beta proteins shows similar results (Supporting Information, Figure S1). The notable feature of the observed highly correlated sequence motifs is that strong correlations are observed at multiple length-scales, with the range of correlations reaching tens and even hundreds of residues. One interesting residue demonstrating strong, long-range correlations is Gly. In particular, there are 65 non-redundant proteins with a large number of repeats containing Gly in each of these proteins. There are 186 different Pfam domains [23] that compose these 65 proteins. However, the most common domain, collagen, is shared only by 4 different proteins out of 65, Table S1. This shows that the observed effect is quite general and not dominated by one particular protein family.

To characterize the sequence correlations further for each group of proteins, we introduce the cumulative correlation function, $H_{\alpha\beta}$,

$$H_{\alpha\beta} = \sum_{x_i \in \max\{\eta_{\alpha\beta}(x_i)\}} \eta_{\alpha\beta}(x_i), \quad \text{Eq. (2)}$$

where the summation is performed at the peaks of $\eta_{\alpha\beta}(x)$. The ratio, $\chi_{\alpha\beta} = H_{\alpha\beta}^{\text{dis}} / H_{\alpha\beta}^{\text{alpha}}$, characterizes the relative correlation strength in disordered proteins as compared with all-alpha proteins, Figure 1B and C (Figure S1, for all-beta proteins). A key observation here is that the diagonal correlations, $\chi_{\alpha\alpha}$, are the strongest. In particular, in disordered proteins the diagonal cumulative correlations are statistically significantly stronger than in all-alpha proteins for G, Y, Q, S, E, R, P, W, C, A, and there is only one amino acid, M, having an opposite trend. Our analytical model predicts below that the observed enhanced strength of diagonal correlations provides the enhanced promiscuity to the sequences.

In order to estimate the effect of sequence correlations on inter-protein promiscuity, we compare the correlation properties of hubs as compared to ‘orphans’ (proteins having no detectable interaction partners), Figure 2A. For ten amino acids, H, F, M, W, G, C, Y, P, I, S, the cumulative sequence correlations in human hubs are statistically significantly stronger than

in orphans. There are no amino acids for which the correlations are stronger in orphans than in hubs. Qualitatively similar, yet quantitatively weaker effect is observed in yeast, with Q, W, C, and P having stronger correlations in hubs than in orphans, and none of amino acids having an opposite trend. In *E.coli* the effect is yet weaker with only two amino acids, C and W having higher correlations in hubs. A notable feature observed in organismal interactomes is that P, C, and W demonstrate strong correlation effect for hubs both in human and yeast, and C and W are shared between all three organisms. We also compared the correlation properties of the entire proteomes in bacteria *E. coli*, yeast *S. Cerevisiae* and human, Figure 2B and C (Figure S2). For nine amino acids, P, H, K, E, R, S, G, A, and Y the diagonal correlations are stronger in the human proteome than in bacteria; and for P the correlations are stronger in human than in yeast with Q having stronger correlations in yeast than in human. This suggests therefore that human and yeast proteomes possess a statistically higher level of protein promiscuity as compared with bacteria.

To answer the question why do sequence correlations lead to the enhanced intra- and inter-protein promiscuity, we developed a simplified biophysical model that captures the effect of sequence correlations on the sequence interaction properties. Formally promiscuity means that the energy spectrum for non-specific binding is shifted towards lower energies. We begin by introducing a simple model for ‘random’ and ‘designed’ (or ‘correlated’) protein-like, linear sequences. For simplicity we use a minimalistic sequence alphabet with two types of residues only. A random sequence is obtained by distributing N_p polar and N_h hydrophobic residues at random within the linear sequence of the total length, $L = N_p + N_h$. Our simplistic approach therefore does not explicitly take into account the folding of the sequence. The average fraction of polar and hydrophobic residues is thus $\phi_{p,0} = N_p / L$ and $\phi_{h,0} = N_h / L$, respectively. In order to obtain a correlated sequence, we allow residues to anneal at a given ‘design’ temperature, T_d . We impose that the residues within the sequence under the design procedure interact through the pairwise additive design potential, $U_{\alpha\beta}(x)$, where $U_{pp}(x)$, $U_{hh}(x)$, and $U_{hp}(x)$ is the interaction potential between polar-polar, hydrophobic-hydrophobic, and hydrophobic-polar residues, respectively. The only two assumptions about the interaction potentials, $U_{\alpha\beta}(x)$, are that they are pairwise additive and have a finite range of action.

Our next step is to analyze the probability distribution $P(E)$ of the interaction energy, E , between the random and correlated sequences. Every pair of interacting sequences consists

of one random and one correlated sequence superimposed in a parallel configuration, thus the problem is a quasi one-dimensional one. The inter-sequence interaction potentials, $V_{pp}(x)$, $V_{hh}(x)$, and $V_{hp}(x)$ can have an arbitrary form. The probability distribution, $P(E)$, is characterized by its mean, $\langle E \rangle$, and by the variance. The mean is independent of the design potential, $U_{\alpha\beta}(x)$, and therefore all the different distributions $P(E)$ obtained at different values of the design temperature, T_d , will have exactly the same mean. The variance, $\sigma^2 = \langle (E - \langle E \rangle)^2 \rangle$, is (Supporting Information):

$$\sigma^2 = 4L\phi_{p,0}\phi_{h,0} \int \frac{dk}{2\pi} |\hat{V}(k)|^2 \frac{1}{1/\phi_{p,0}\phi_{h,0} + \hat{U}(k)/k_B T_d}, \quad \text{Eq. (3)}$$

where $\hat{U}(k) = \int U(x)e^{ikx} dx$, and $U(x) = U_{pp}(x) + U_{hh}(x) - 2U_{ph}(x)$, and analogously for $\hat{V}(k)$. The larger σ , and thus the broader the distribution, $P(E)$, the more promiscuous are the correlated sequences. The analysis of Eq. (3) leads to the two key conclusions. First, the more negative is the ‘design’ potential, $U(x)$, the larger is σ . Taking into account the definition of $U = U_{pp} + U_{hh} - 2U_{ph}$, one concludes that in order to increase σ one needs to design the sequences with the enhanced correlations in the positions between the residues of similar types. This means that correlated sequences where residues of the same type are clustered together will be the more promiscuous ones. Second, such correlated sequences will interact statistically stronger (than non-correlated sequences) with any set of arbitrary sequences independently on the sign of the inter-residue interaction potential, $V(x)$, Eq. (3). The predicted effects therefore are generic and qualitatively independent of the specific form of the inter-residue interaction potentials and on the amino acid composition of sequences. Intuitively, stronger correlations correspond to repetitive sequence patterns with a longer correlation length. The properties of the correlated patterns depend critically on the sign of the interaction potentials, $U_{\alpha\beta}(x)$, used in the design procedure. If the effective design potential $U(x)$ is overall negative (this corresponds to the attraction between the amino acids of similar types), the correlated patterns will have the form of repetitive residues of the same type, for example: HHHHPPPPHHHPPP... For entirely uncorrelated (random) sequences, all the matrix elements of $\eta_{\alpha\beta}(x)$ are equal to unity. The clustering of residues of similar types corresponds to $\eta_{\alpha\alpha}(x) > 1$, Figure 3. We computed $P(E)$ at different values of T_d and we represented the results as a ratio between the dispersion, σ , and the dispersion of the

corresponding probability distribution when both interacting sequences are entirely random, $\sigma_{r,r}$. In accordance with the analytical predictions, $\sigma > \sigma_{r,r}$, Figure 3. A key message is that the enhanced correlations between amino acids of the same type lead to the broadening of the distribution, $P(E)$. Such broadening implies that the corresponding extreme value distribution (EVD) will always be shifted to lower energies for stronger correlated sequences [24]. The latter property implies that such correlated sequences will be more promiscuous, *i.e.* statistically prone to a stronger binding with an arbitrary sequence.

We stress that the presented simplified model does not explicitly take into account protein folding and, therefore, underestimates the effect of longer-range sequence correlations induced by the presence of a protein chain. Taking protein folding into account properly should provide an additional insight into the effect of long-range sequence correlations on protein structural disorder. Elucidation of the latter issue is the subject of our future work.

Discussion

We note that consistent with our predictions, it was observed recently in [21] that homo-oligomer repeats are overrepresented in human, chimp, mouse, rat, and chicken genomes. Remarkably, seven highly correlated residues observed in our analysis of disordered proteins: G, Q, S, E, R, P, and A, also appear among the residues forming frequent oligomer repeats observed in [21]. One interesting example of highly correlated protein is titin, 2MDa_1, Figures S3 and S4. This long protein with 18,534 amino acids contains 41 immunoglobulin I-set domains and 9 fibronectin Fn3 domains. However, the correlation analysis shows that the strongest correlations come from the 6000 amino acids long inter-domain region, Figure S4. This region does not contain any immunoglobulin and fibronectin domains, but yet demonstrates the strongest diagonal correlations.

We stress that a key prediction of the model is that highly promiscuous sequences possess strong diagonal correlations, $\eta_{\alpha\alpha}(x) > 1$, and at the same time, weak off-diagonal correlations, $\eta_{\alpha\beta}(x) < 1$, Figure 3A. Remarkably, we observe qualitatively similar behavior in the off-diagonal correlation functions of disordered proteins, Figure 4. In the examples presented in Figure 4 we show that the off-diagonal correlation functions are significantly reduced, $\eta_{\alpha\beta}(x) < 1$, for amino acids demonstrating strong diagonal correlations, such as Q, S, P, E, R, and A. Intuitively, strong diagonal correlations correspond to homo-oligomer repeats within protein sequences. Such repeats represent the most promiscuous sequences according to

our model. It is known that many proteins involved in neurodegenerative diseases are mutated in a way that expands the length of repeated sequence regions. One of the most prominent examples is the huntingtin protein involved in the Huntington's disease [25]. This protein has numerous repeats such as polyQ and polyP and it is known that the extended polyQ mutants are prone to aggregation [25].

In summary, here we suggest a mechanism that explains why sequence repeats lead to enhanced protein promiscuity. We predict that both enhanced structural disorder and enhanced non-specific binding arise due to the enhancement of diagonal correlations of amino acids within protein sequences. This statistical effect is driven by symmetry properties of sequences and hence it is qualitatively robust with respect to the parameters of the system, such as amino acid composition and specific form of the interaction potentials.

Materials and Methods

Disordered proteins dataset

To compute sequence correlations in disordered proteins, we used the database of disordered proteins DisProt 5.1 [22], <http://www.disprot.org/>. From this database, we selected a set of 417 non-redundant proteins with a mutual, pairwise sequence identity of less than 25%, Table S2. We computed sequence correlations without aligning the sequences. In order to remove the bias, we did not include in our statistical correlation analysis the longest protein, titin (2MDa_1), with the length of 18,534 amino acids. We analyzed the correlation properties of this protein separately, Figures S3 and S4.

All-alpha and all-beta proteins dataset

We selected the non-redundant sequences of all-alpha and all-beta proteins (with a pairwise sequence identity of less than 30%) from the Astral database [26], <http://astral.berkeley.edu/>. We used a set of 1468 all alpha and 1339 all beta proteins, respectively, with the total sequence length equal approximately to the total sequence length of the disordered protein set.

Hubs and orphans in human, yeast, and bacterial proteomes

Human: We used the yeast two-hybrid (Y2H) PPI data [6]. Hubs were defined as proteins having 10 or more binding partners. Orphans were defined as proteins for which no interactions were detected. There were total of 107 hubs and 120 orphans, Table S3. **Yeast:** We used the PPI dataset from [4] with a similar definition of hubs and orphans as in the human PPI dataset. There were total 590 hubs and 891 orphans, Table S4. ***E. coli:*** We used

the PPI dataset from [5] for the K-12 strain W3110 with 277 hubs and 374 orphans, Table S5. In each of the three organisms the total sequence length of hubs was approximately equal to the total sequence length of orphans. In each organism the mutual, pairwise sequence identity in hubs and orphans was imposed to be less than 75%.

Entire proteome data

The entire proteome sequences for human, yeast and *E. coli* (strain K-12, W3110) were downloaded from the NCBI site, <http://www.ncbi.nlm.nih.gov/guide/genomes-maps/>. Each proteome was filtered from redundant proteins to reach the mutual, pairwise sequence identity of less than 40%. This left us with 12,033, 5112, and 3683 proteins in human, yeast, and *E. coli*, respectively.

Analysis of sequence correlations

In order to compute the average, $\langle g_{\alpha\beta}^r(x) \rangle$, in Eq. (1), we used five randomized replicas for each protein sequence. All presented correlation functions, $\eta_{\alpha\beta}(x)$, are computed with respect to the entire set of non-aligned protein sequences in a given group (*e.g.* disordered proteins, hubs, orphans, entire proteomes for each organism, *etc.*). In order to compute the cumulative correlation functions, $H_{\alpha\beta}$, we have performed a summation with respect to five largest peaks of $\eta_{\alpha\beta}(x)$ in Eq. (2). In our estimates of amino acids with significantly overrepresented correlation strength, we used a 10% threshold for the relative correlation strength, $\chi_{\alpha\alpha}$. If thus $\chi_{\alpha\alpha} > 1.1$, we assigned α to a set of significantly correlated amino acids.

Analytical theory

The details of the analytical theory and the derivation of Eq. (3) are presented in Supporting Information.

Acknowledgements

We thank Amir Aharoni, Gilad Haran, Nikolaus Rajewsky, Irit Sagi, Eugene Shakhnovich, and the members of Marc Vidal's lab for helpful discussions.

References

1. Dyson HJ, Wright PE (2005) Intrinsically unstructured proteins and their functions. *Nat Rev Mol Cell Biol* 6: 197-208.
2. Khersonsky O, Roodveldt C, Tawfik DS (2006) Enzyme promiscuity: evolutionary and mechanistic aspects. *Current Opinion in Chemical Biology* 10: 498-508.

3. Nobeli I, Favia AD, Thornton JM (2009) Protein promiscuity and its implications for biotechnology. *Nat Biotechnol* 27: 157-167.
4. Batada NN, Reguly T, Breitkreutz A, Boucher L, Breitkreutz BJ, et al. (2006) Stratus not altocumulus: a new view of the yeast protein interaction network. *PLoS Biol* 4: e317.
5. Hu P, Janga SC, Babu M, Diaz-Mejia JJ, Butland G, et al. (2009) Global functional atlas of *Escherichia coli* encompassing previously uncharacterized proteins. *PLoS Biol* 7: e96.
6. Rual JF, Venkatesan K, Hao T, Hirozane-Kishikawa T, Dricot A, et al. (2005) Towards a proteome-scale map of the human protein-protein interaction network. *Nature* 437: 1173-1178.
7. Gavin AC, Aloy P, Grandi P, Krause R, Boesche M, et al. (2006) Proteome survey reveals modularity of the yeast cell machinery. *Nature* 440: 631-636.
8. Bork P, Jensen LJ, von Mering C, Ramani AK, Lee I, et al. (2004) Protein interaction networks from yeast to human. *Curr Opin Struct Biol* 14: 292-299.
9. Haynes C, Oldfield CJ, Ji F, Klitgord N, Cusick ME, et al. (2006) Intrinsic disorder is a common feature of hub proteins from four eukaryotic interactomes. *PLoS Comput Biol* 2: e100.
10. Kim PM, Sboner A, Xia Y, Gerstein M (2008) The role of disorder in interaction networks: a structural analysis. *Mol Syst Biol* 4: 179.
11. Cornette JL, Margalit H, Berzofsky JA, DeLisi C (1995) Periodic variation in side-chain polarities of T-cell antigenic peptides correlates with their structure and activity. *Proc Natl Acad Sci U S A* 92: 8368-8372.
12. Eisenberg D, Weiss RM, Terwilliger TC (1984) The hydrophobic moment detects periodicity in protein hydrophobicity. *Proc Natl Acad Sci U S A* 81: 140-144.
13. Marcotte EM, Pellegrini M, Yeates TO, Eisenberg D (1999) A census of protein repeats. *J Mol Biol* 293: 151-160.
14. Rackovsky S (1998) "Hidden" sequence periodicities and protein architecture. *Proc Natl Acad Sci U S A* 95: 8580-8584.
15. Rosato V, Pucello N, Giuliano G (2002) Evidence for cysteine clustering in thermophilic proteomes. *Trends Genet* 18: 278-281.
16. Xiong H, Buckwalter BL, Shieh HM, Hecht MH (1995) Periodicity of polar and nonpolar amino acids is the major determinant of secondary structure in self-assembling oligomeric peptides. *Proc Natl Acad Sci U S A* 92: 6349-6353.
17. Dosztanyi Z, Chen J, Dunker AK, Simon I, Tompa P (2006) Disorder and sequence repeats in hub proteins and their implications for network evolution. *J Proteome Res* 5: 2985-2995.
18. Jorda J, Xue B, Uversky VN, Kajava AV (2010) Protein tandem repeats - the more perfect, the less structured. *FEBS J* 277: 2673-2682.
19. Tompa P (2003) Intrinsically unstructured proteins evolve by repeat expansion. *Bioessays* 25: 847-855.
20. Lise S, Jones DT (2005) Sequence patterns associated with disordered regions in proteins. *Proteins* 58: 144-150.
21. Simon M, Hancock JM (2009) Tandem and cryptic amino acid repeats accumulate in disordered regions of proteins. *Genome Biol* 10: R59.
22. Sickmeier M, Hamilton JA, LeGall T, Vacic V, Cortese MS, et al. (2007) DisProt: the Database of Disordered Proteins. *Nucleic Acids Res* 35: D786-793.
23. Finn RD, Mistry J, Tate J, Coghill P, Heger A, et al. The Pfam protein families database. *Nucleic Acids Res* 38: D211-222.
24. Lukatsky DB, Shakhnovich EI (2008) Statistically enhanced promiscuity of structurally correlated patterns. *Phys Rev E Stat Nonlin Soft Matter Phys* 77: 020901.

25. Cohen E, Dillin A (2008) The insulin paradox: aging, proteotoxicity and neurodegeneration. *Nat Rev Neurosci* 9: 759-767.
26. Chandonia JM, Hon G, Walker NS, Lo Conte L, Koehl P, et al. (2004) The ASTRAL Compendium in 2004. *Nucleic Acids Res* 32: D189-192.

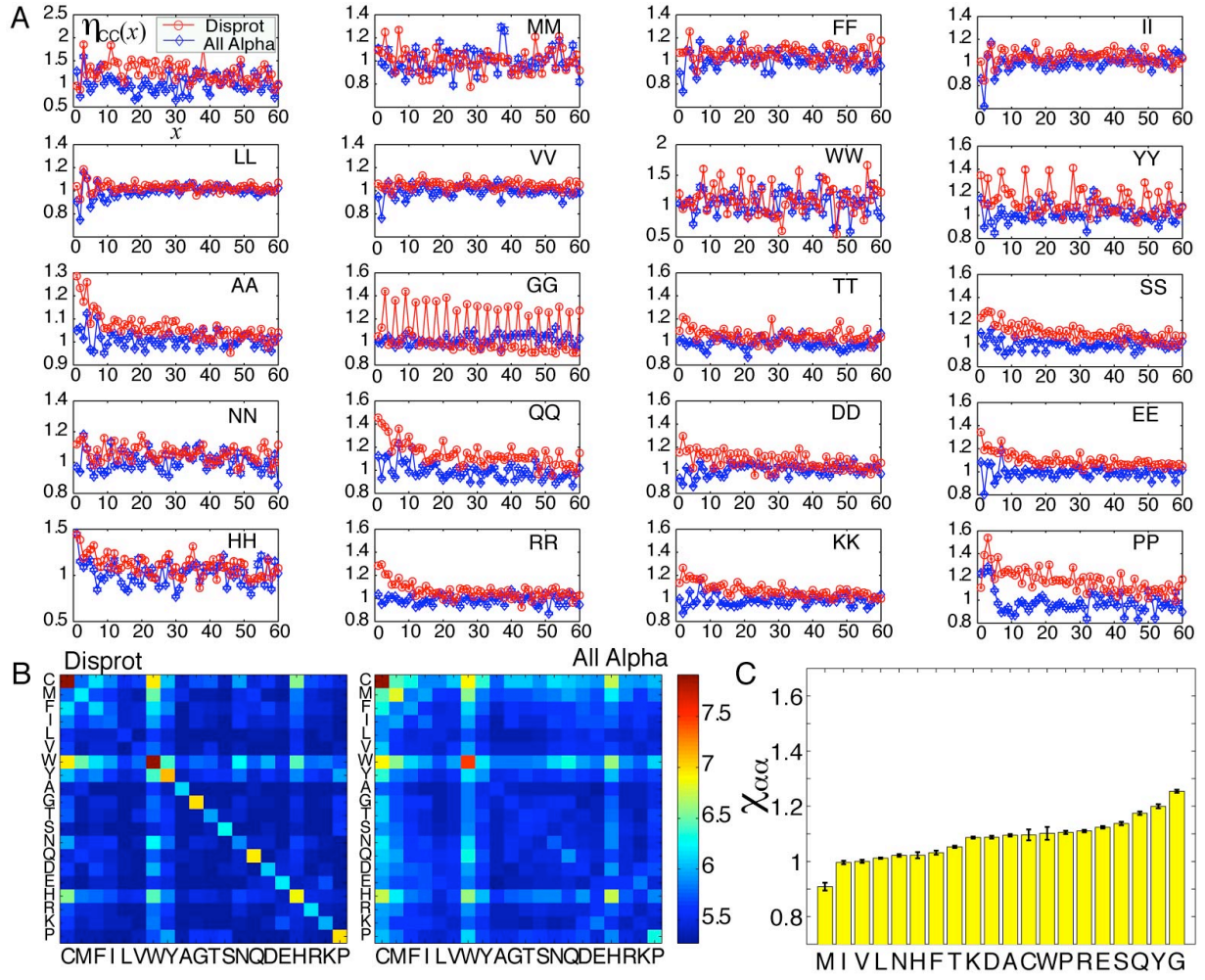


Figure 1: **A.** Diagonal elements of the correlation function, $\eta_{\alpha\alpha}(x)$, for all 20 types of amino acids for intrinsically disordered protein (red circles) and all-alpha proteins (blue diamonds). **B.** The heat-map representation of the entire cumulative correlations matrix, $H_{\alpha\beta}$, for disordered, and all-alpha proteins. **C.** The diagonal elements of the ratio, $\chi_{\alpha\alpha} = H_{\alpha\beta}^{\text{dis}} / H_{\alpha\beta}^{\text{alpha}}$.

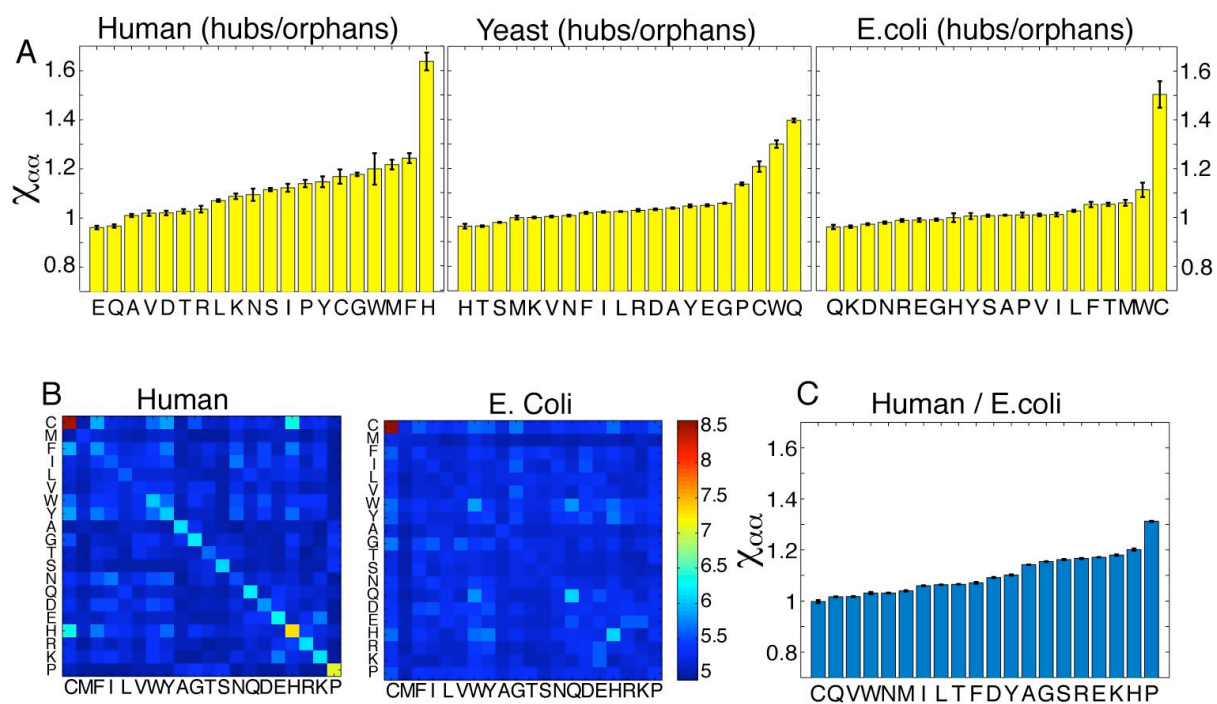


Figure 2: **A.** Relative correlation strength of hubs as compared with orphans, $\chi_{\alpha\alpha} = H_{\alpha\alpha}^{\text{hubs}} / H_{\alpha\alpha}^{\text{orphans}}$, for human, yeast, and *E. coli*, respectively. **B.** The cumulative correlation matrix, $H_{\alpha\beta}$, for the entire human and *E. coli* proteomes, respectively. **C.** Relative correlation strength, $\chi_{\alpha\alpha} = H_{\alpha\alpha}^{\text{human}} / H_{\alpha\alpha}^{\text{ecoli}}$, of diagonal correlations of the entire human as compared with the entire *E. coli* proteomes.

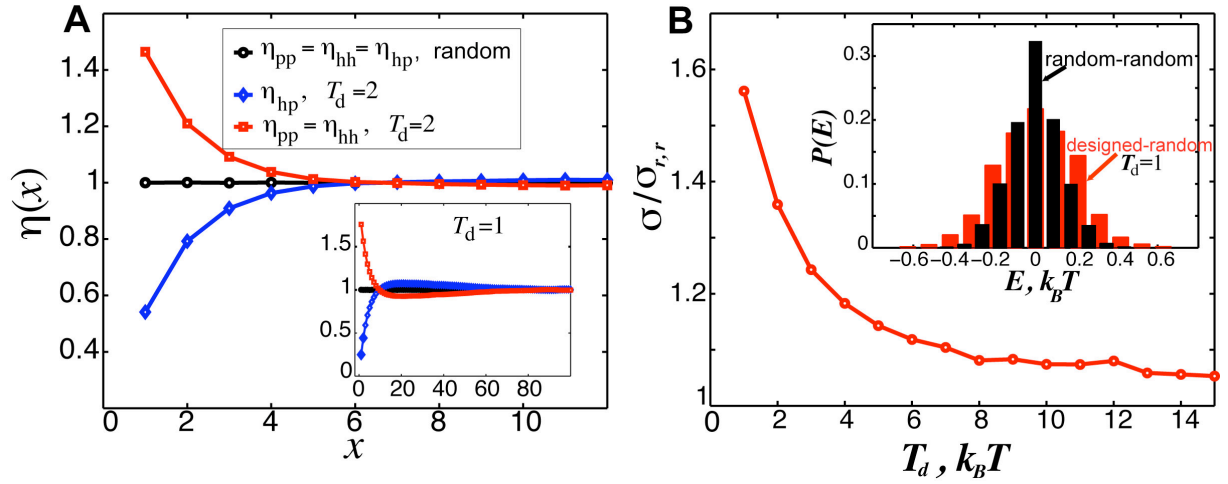


Figure 3: **A.** Computed sequence correlation functions for the ‘designed’ sequences, $\eta_{pp}(x) = \eta_{hh}(x)$ (red squares), $\eta_{hp}(x) = \eta_{ph}(x)$ (blue diamonds); and for the random sequences, (black circles). The design potential was chosen to be $U_{pp} = U_{hh} = -1$, and $U_{hp} = 1$, and we assumed that only the nearest-neighbor residues can interact. The design temperature is $T_d = 2$. The sequence length was chosen to be 200 amino acids, and we generated 5000 different sequences in each calculation. The uniform amino acid composition was adopted: 50% polar (p) and 50% hydrophobic (h) residues in each sequence. The error bars are smaller than the symbol size. Insert: an analogous computation as in the main figure but at a lower design temperature, $T_d = 1$. **B.** Computed ratio between the dispersions of the $P(E)$ for the interaction energies of the designed-random, σ , and random-random, $\sigma_{r,r}$, sequence pairs at different values of the design temperature. The error bars are smaller than the symbol size. Insert: Computed probability distribution function, $P(E)$, for the interaction energies between the pairs of two random sequences (black), and pairs consisting each of a random and a designed sequences, where the designed sequences were generated at $T_d = 1$ (red). The energy E is normalized per one residue.

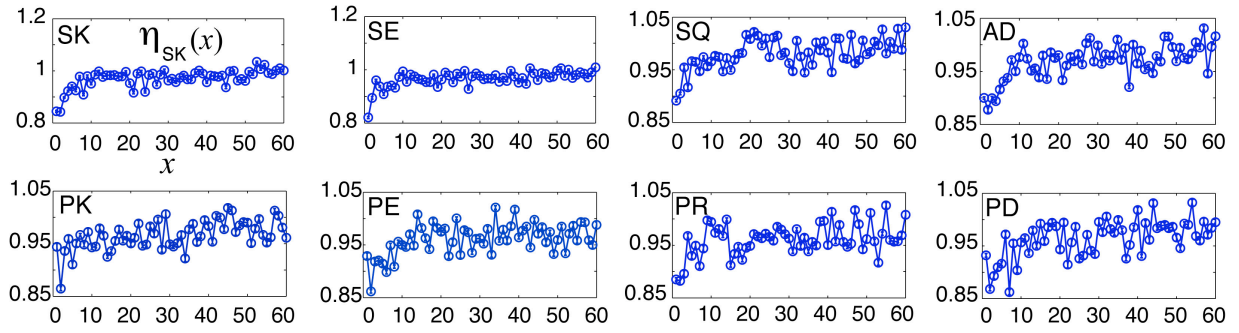


Figure 4: Example: computed off-diagonal elements of the correlation functions, $\eta_{\alpha\beta}(x)$, for structurally disordered protein dataset. These correlation functions behave in a qualitative agreement with the behavior predicted for the off-diagonal elements of $\eta_{\alpha\beta}(x)$ in the model promiscuous sequences, Figure 3A, where $\eta_{\alpha\beta}(x) < 1$.

Supporting Information

Multi-scale sequence correlations increase proteome structural disorder and promiscuity

Ariel Afek and David B. Lukatsky

Department of Chemistry, Ben-Gurion University of the Negev, Beer-Sheva 84105 Israel

1. Statistically enhanced promiscuity of correlated sequences

Here we provide the details of the analytical model for interacting correlated sequences. As described in the main text, we first generate random, linear sequences with a given amino acid composition. After each random sequence is generated, the residues are fixed and not allowed to change their positions. A correlated sequence is obtained using the following stochastic, Monte-Carlo (MC) procedure. We start with a random sequence and allow amino acids to anneal at a given ‘design’ temperature, T_d . We note that our notion of ‘designed’ sequences stands to describe the existence of positional correlations of amino acids within the linear sequences and not the folding. We thus impose that the residues within the sequence under the design procedure interact through the pair-wise additive design potential, $U_{\alpha\beta}(x)$. The intra-sequence interaction energy for any given residue distribution is thus:

$$\begin{aligned} E_{\text{intra}} &= \frac{1}{2} \int \phi_p(x) U_{pp}(x-x') \phi_p(x') dx dx' \\ &+ \frac{1}{2} \int \phi_h(x) U_{hh}(x-x') \phi_h(x') dx dx' \\ &+ \int \phi_h(x) U_{hp}(x-x') \phi_p(x') dx dx' \end{aligned} \quad \text{Eq. (S1)}$$

where $\phi_p(x)$ and $\phi_h(x)$ are the local, linear fraction densities of polar and hydrophobic residues, respectively. The average composition of polar and hydrophobic residues is fixed by the values, $\phi_{p,0} = N_p / L$ and $\phi_{h,0} = N_h / L$, respectively, and we impose that the total fraction of residues at each sequence position, x , is unity, $\phi_p(x) + \phi_h(x) = 1$. Here $U_{pp}(x)$, $U_{hh}(x)$, and $U_{hp}(x) = U_{ph}(x)$ is the interaction potential between polar-polar, hydrophobic-hydrophobic, and hydrophobic-polar residues, respectively. We also note that $\phi_p(x)$ can be represented in

the form: $\phi_p(x) = \phi_{p,0} + \delta\phi_p(x)$, where $\delta\phi_p(x)$ is the deviation of the local density of polar residues from its average value, and analogously, $\phi_h(x) = \phi_{h,0} + \delta\phi_h(x)$. The only two assumptions about the interaction potentials, $U_{\alpha\beta}(x)$, used in the sequence design procedure are that they are pair-wise additive and have a finite range of action.

Every pair of interacting sequences consists of one random and one correlated sequence superimposed in a parallel configuration, thus the problem is a quasi one-dimensional one. Our key message is that the enhanced correlations between amino acids of the same type lead to the broadening of the distribution, $P(E)$. Such broadening implies that the corresponding extreme value distribution (EVD) will always be shifted towards lower energies for stronger correlated sequences (Lukatsky and Shakhnovich, 2008). This implies that such correlated sequences will be statistically prone to a stronger binding with an arbitrary sequence. We call the latter property ‘promiscuity’. We use an ensemble of entirely random sequences as a proxy for an ensemble of arbitrary protein sequences. The interaction energy between the random and correlated sequences is:

$$E = \int v_p(x)V_{pp}(x-x')\phi_p(x')dx dx' + \int v_h(x)V_{hh}(x-x')\phi_h(x')dx dx' + \int v_h(x)V_{hp}(x-x')\phi_p(x')dx dx' + \int v_p(x)V_{hp}(x-x')\phi_h(x')dx dx' \quad \text{Eq. (S2)}$$

where $v_p(x)$ and $v_h(x)$ are the local, linear fraction densities of polar and hydrophobic residues, respectively, within the random sequence, and here again $v_p(x) + v_h(x) = 1$, and $v_p(x) = \phi_{p,0} + \delta v_p(x)$ with $\delta v_p(x)$ being the deviation of the polar residue density from its average value, and analogously for $v_h(x) = \phi_{h,0} + \delta v_h(x)$. We thus assume that the average amino acid composition is the same for random and correlated sequences. We emphasize that the inter-sequence interaction potentials, $V_{pp}(x)$, $V_{hh}(x)$, and $V_{hp}(x) = V_{ph}(x)$ need not be identical to the potentials $U_{pp}(x)$, $U_{hh}(x)$, and $U_{hp}(x) = U_{ph}(x)$ used in the sequence design procedure.

The probability distribution for the interaction energies between the random and correlated sequences, $P(E)$, is characterized by its mean, $\langle E \rangle$, and by the variance, σ^2 . The mean, $\langle E \rangle$, is independent on the design potential, $U_{\alpha\beta}(x)$, and therefore all the different distributions $P(E)$ obtained at different values of the design temperature, T_d , will have exactly the same mean. The variance of $P(E)$ is $\sigma^2 = \langle (E - \langle E \rangle)^2 \rangle$, where the only relevant term for the averaging is quadratic in the sequence density fluctuations:

$$\delta E_2 = \int \delta v_p(x) V(x-x') \delta \phi_p(x') dx dx' , \quad \text{Eq. (S3)}$$

where $V(x) = V_{pp}(x) + V_{hh}(x) - 2V_{ph}(x)$, and $\hat{V}(k) = \int V(x) e^{-ikx} dx$. The averaging in σ is performed using the Boltzmann probability distribution function for the sequence density fluctuations of the correlated (*i.e.* designed) sequences that has the following form:

$$P_d[\delta \phi_p(x)] = C_1 \exp \left[- \int \frac{\delta \phi_p^2(x)}{2\phi_{p,0}\phi_{h,0}} dx \right] \exp(-E_{\text{intra}}/k_B T_d) \quad \text{Eq. (S4)}$$

where T_d is the design temperature, and k_B is the Boltzmann constant. The first exponential term in Eq. (S4) is the entropic contribution due to the sequence density fluctuations of the ‘designed’ sequences, and the second exponential term represents the strength of the correlations within the ‘designed’ sequences. The corresponding probability distribution for the density fluctuations of the random sequences contains only the entropic contribution:

$$P_r[\delta v_p(x)] = C_2 \exp \left[- \int \frac{\delta v_p^2(x)}{2\phi_{p,0}\phi_{h,0}} dx \right]. \quad \text{Eq. (S5)}$$

The constants C_1 and C_2 in Eqs. (4) and (5), are found from the normalization constrains applied on the probability distributions. The averaging leads to the following result:

$$\sigma^2 = 4L\phi_{p,0}\phi_{h,0} \int \frac{dk}{2\pi} |\hat{V}(k)|^2 \frac{1}{1/\phi_{p,0}\phi_{h,0} + \hat{U}(k)/k_B T_d}, \quad \text{Eq. (S6)}$$

where $\hat{U}(k) = \int \hat{U}(x) e^{-ikx} dx$, and $U(x) = U_{pp}(x) + U_{hh}(x) - 2U_{ph}(x)$. The larger σ is (and thus the broader is the distribution $P(E)$ of the interaction energies between the correlated and random sequences), the more promiscuous are the correlated sequences. We note that our model is only solvable analytically in the Gaussian approximation, and not exactly solvable, unlike the one-dimensional Ising model, due to the generally long-range nature of the intra-sequence (‘design’) potential, $U(x)$, and the inter-sequence potential, $V(x)$. We also note the existence of the singularity in Eq. (S6) at sufficiently large and negative values of the ‘design’ potential, $U(x)$, when the Gaussian fluctuation model breaks down.

The analysis of Eq. (S6) shows that the more negative is the ‘design’ potential, $U(x)$, the larger is σ . Taking into account the definition of $U(x) = U_{pp}(x) + U_{hh}(x) - 2U_{ph}(x)$, one concludes that in order to increase σ one needs to design the sequences with the enhanced correlations in the positions between the residues of similar types. This means that correlated

sequences where residues of the same type are clustered together will be the more promiscuous ones. Ones such correlated sequences are produced, they will interact statistically stronger (than non-correlated sequences would do) with any arbitrary sequences independently on the sign of the inter-residue interaction potential, $V(x) = V_{pp}(x) + V_{hh}(x) - 2V_{ph}(x)$. We emphasize that the predicted effects are generic and qualitatively independent on the specific form of the inter-residue interaction potentials and on the amino acid composition of the sequences.

We note that the predicted effect gets even stronger when both interacting sequences are ‘designed’ (*i.e.* correlated). In the latter case the variance, $\sigma_{d,d}$, of the corresponding $P(E)$ is a straightforward generalization of Eq. (S6):

$$\sigma_{d,d}^2 = 4L \int \frac{dk}{2\pi} |\hat{V}(k)|^2 \frac{1}{(1/\phi_{p,0}\phi_{h,0} + \hat{U}_1(k)/k_B T_{d1})(1/\phi_{p,0}\phi_{h,0} + \hat{U}_2(k)/k_B T_{d2})}, \quad \text{Eq. (S7)}$$

where $U_1(x)$ and $U_2(x)$ are defined analogously to $U(x)$ for each of the interacting sequences; T_{d1} and T_{d2} are the design temperatures for the first and second sequence, respectively. If both ‘design’ potentials, $U_1(x)$ and $U_2(x)$, are overall negative, then $\sigma_{d,d} > \sigma$, and thus in the latter case the sequences will be statistically more promiscuous than in the case when only one of the interacting sequences is ‘designed’ (Eq. (S6)). We stress that the interacting sequences are designed independently and not optimized in any way towards a stronger binding. Therefore the observed effect of statistically enhanced binding refers to the non-specific (promiscuous) binding.

References

Lukatsky DB, Shakhnovich EI (2008) Statistically enhanced promiscuity of structurally correlated patterns. *Phys Rev E Stat Nonlin Soft Matter Phys* **77**: 020901.

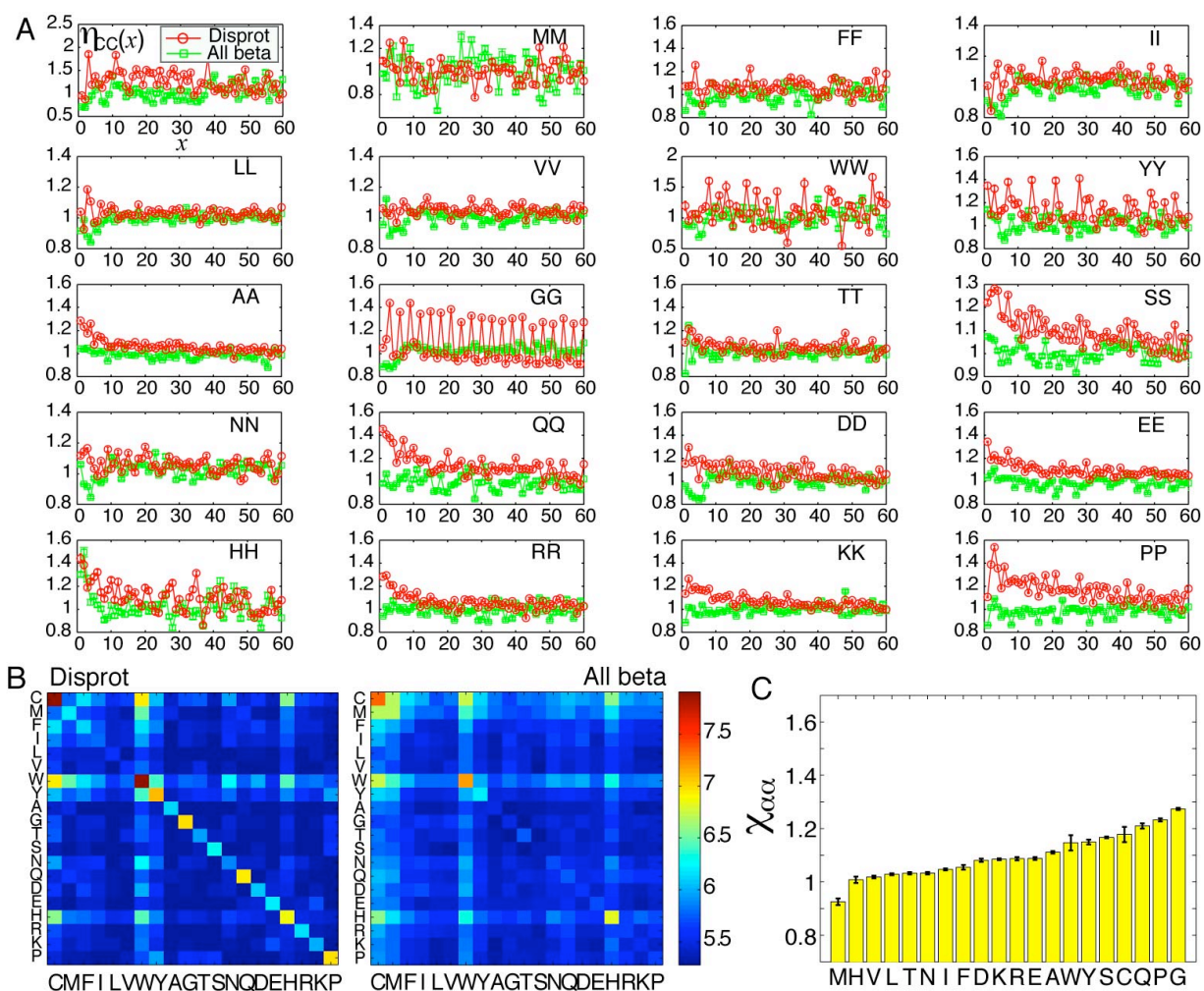


Figure S1: This figure is analogous to Figure 1 of the main text. **A.** Diagonal elements of the correlation function, $\eta_{\alpha\alpha}(x)$, for intrinsically disordered proteins (red circles) compared with all-beta proteins (green squares). **B.** The heat-map representation of the entire cumulative correlation matrix $H_{\alpha\beta}$, for disordered, and all-beta proteins, respectively. **C.** The diagonal elements of the ratio, $\chi_{\alpha\alpha} = H_{\alpha\beta}^{\text{dis}} / H_{\alpha\beta}^{\text{beta}}$. The details for the protein datasets used in the computation are described in Materials and methods. There are eight amino acids, G, P, Q, C, S, Y, W, and A, with significantly stronger correlations in disordered proteins as compared with all-beta proteins. There are no amino acids with an opposite trend.

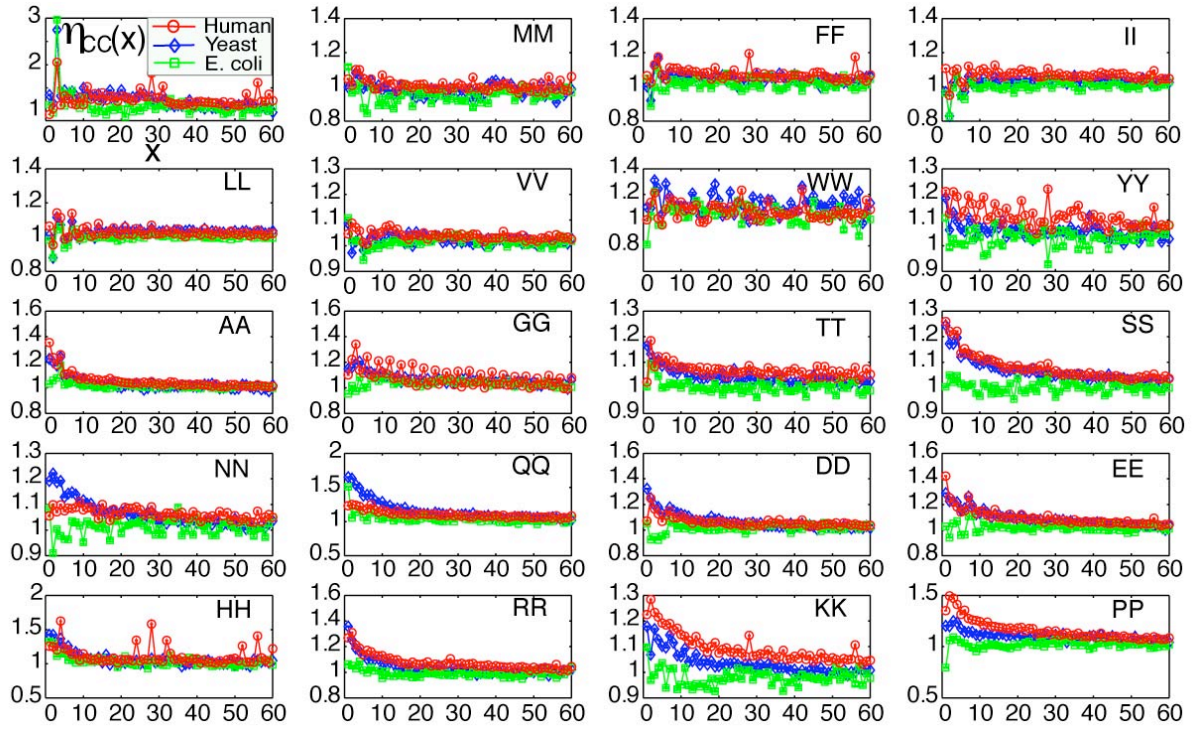


Figure S2: Diagonal elements of the correlation function, $\eta_{aa}(x)$, for the entire human (red circles), yeast (blue diamonds), and *E. Coli* (green squares) proteomes. Each proteome was filtered from redundant proteins to reach the mutual, pair-wise sequence identity of less than 40% (see Materials and methods).

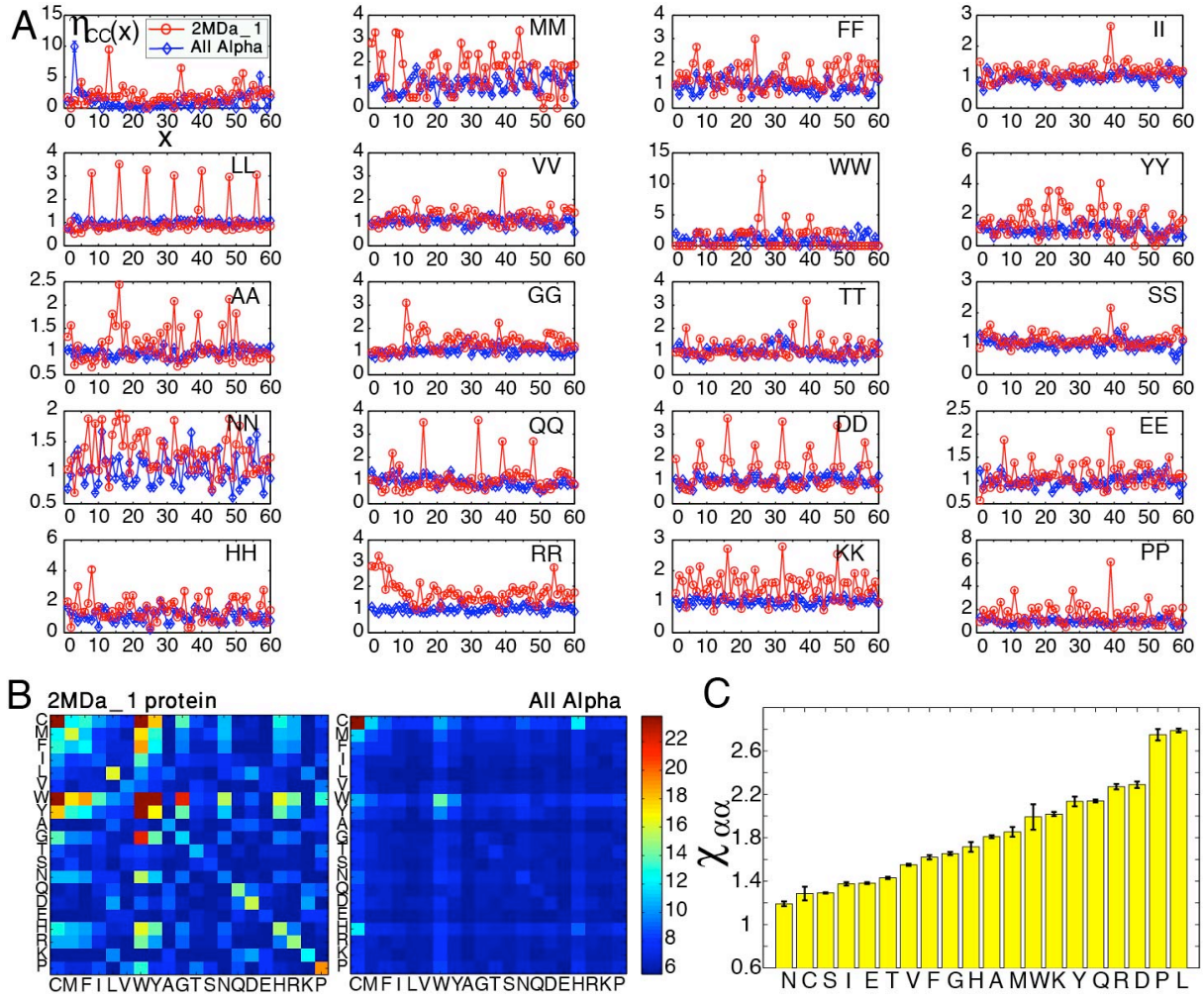


Figure S3: Computed correlation properties of titin (2MDa_1, Q8ISF7_CAEEL) from DisProt 5.1 database. Protein size 18,534 amino acids. **A.** Diagonal elements of the correlation function, $\eta_{\alpha\alpha}(x)$, for 2MDa_1 (red circles) compared with all-alpha proteins (blue diamonds). In the computation, we used 196 all-alpha proteins with the total sequence length approximately equal to the sequence length of 2MDa_1. **B.** The heat-map representation of the entire cumulative correlation matrix $H_{\alpha\beta}$, for titin, 2MDa_1, and all-alpha proteins, respectively. **C.** The diagonal elements of the ratio, $\chi_{\alpha\alpha} = H_{\alpha\beta}^{2MDa_1} / H_{\alpha\beta}^{\alpha}$. All amino acids in titin are significantly strongly correlated than in all-alpha proteins.

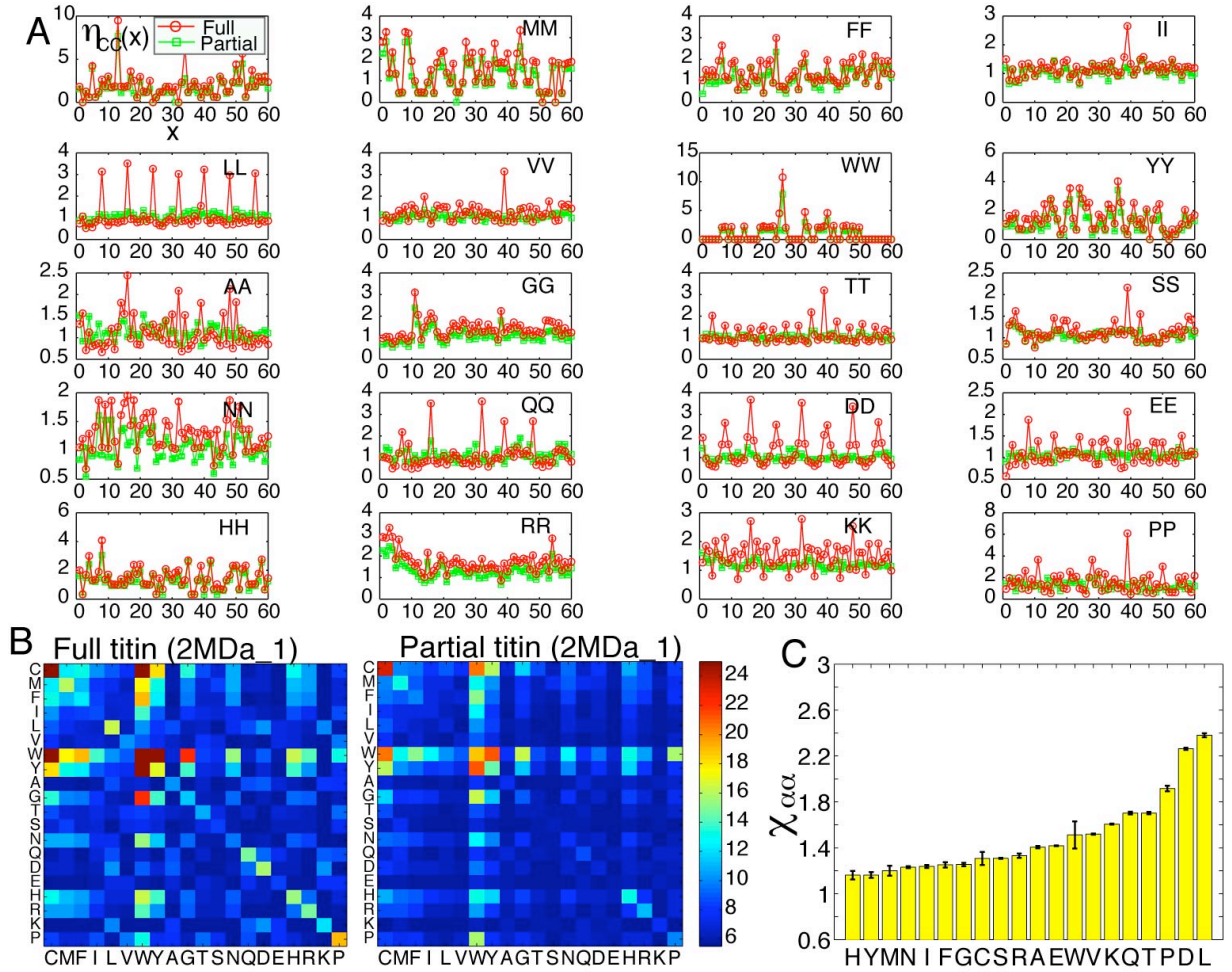


Figure S4: **A.** Computed correlation properties of full titin (2MDa_1, Q8ISF7_CAEEL) (red circles) as compared with full titin with the removed inter-domain part of 6137 amino acids (we denoted the latter sequence as partial titin 2MDa_1) (green squares). The removed inter-domain part is located between the immunoglobulin (I-set) and the fibronectin (Fn3) domains and contains no other recognizable Pfam structural domains. After this inter-domain sequence is removed the correlation strength, $\eta_{\alpha\alpha}(x)$, of the remaining sequence is dramatically reduced. **B.** The heat-map representation of the entire cumulative correlation matrix $H_{\alpha\beta}$, for titin 2MDa_1 and for partial 2MDa_1, respectively. **C.** The diagonal elements of the ratio, $\chi_{\alpha\alpha} = H_{\alpha\beta}^{2MDa_1} / H_{\alpha\beta}^{partial_2MDa_1}$. All amino acids in full titin are significantly strongly correlated as compared with partial titin. The effect is particularly strong for diagonal correlations. A key message is that most of the correlations come from the region of the sequence not associated with any known domains, and not from the regions containing repeated structural domains.

| Pfam | Disprot ID | Number of domain repeats in protein | Number of proteins |
|--------------------------------|------------------------------------|--|---------------------------|
| AAA | DP00435 | X2 | 1 |
| ACC_central | DP00557 | | 1 |
| Agenet | DP00134 | | 1 |
| AIG1 | DP00610 | | 1 |
| Ald_Xan_dh_C | DP00450 | | 1 |
| Ald_Xan_dh_C2 | DP00450 | | 1 |
| Ank | DP00467 | X20 | 1 |
| Anthrax_toxA | DP00591 | | 1 |
| APC_15aa | DP00519 | X4 | 1 |
| APC_basic | DP00519 | | 1 |
| APC_crr | DP00519 | X6 | 1 |
| Arm | DP00341, DP00519 | X5, X3 | 2 |
| B1 | DP00121 | X5 | 1 |
| Biotin_carb_C | DP00557 | | 1 |
| Biotin_lipoyl | DP00557 | | 1 |
| Bromodomain | DP00081, DP00348 | X2 | 2 |
| BTB | DP00328 | | 1 |
| C1q | DP00569 | | 1 |
| Ca_chan_IQ | DP00228 | | 1 |
| Carboxyl_trans | DP00557 | | 1 |
| CARD | DP00554 | | 1 |
| CDC48_2 | DP00435 | | 1 |
| CDC48_N | DP00435 | | 1 |
| CITED | DP00356 | X2 | 1 |
| Cloacin | DP00342 | | 1 |
| Cna_B | DP00065, DP00098 | X5, X7 | 2 |
| CO_deh_flav_C | DP00450 | | 1 |
| COLFI | DP00274 | | 1 |
| Collagen | DP00246, DP00274, DP00460, DP00569 | X2, X9 | 4 |
| Collagen_bind | DP00098 | | 1 |
| CPSase_L_chain | DP00557 | | 1 |
| CPSase_L_D2 | DP00557 | | 1 |
| Creb_binding | DP00348 | | 1 |
| DEAD | DP00560 | | 1 |
| Death | DP00467 | | 1 |
| Dehydrin | DP00530 | | 1 |
| DnaJ | DP00351 | | 1 |
| DSL | DP00418 | | 1 |
| DUF1865 | DP00573 | | 1 |
| DUF3406 | DP00610 | | 1 |
| DUF3409 | DP00675 | | 1 |
| DUF3591 | DP00081 | | 1 |
| DUF902 | DP00348 | | 1 |
| E1-E2_ATPase | DP00282 | | 1 |
| E2R135 | DP00342 | | 1 |
| EB1_binding | DP00519 | | 1 |

| | | | |
|---------------------------------|------------------------------|--------|---|
| EGF | DP00418 | | 1 |
| EGF 2 | DP00418 | | 1 |
| Egfpox | DP00418, DP00623 | X10 | 2 |
| Egfcx | DP00418 | | 1 |
| FAD_binding_5 | DP00450 | | 1 |
| FCP1_C | DP00177 | | 1 |
| Fer2 | DP00450 | | 1 |
| Fer2_2 | DP00450 | | 1 |
| FERM_M | DP00653 | | 1 |
| FERM_N | DP00653 | | 1 |
| Fib_alpha | DP00233 | | 1 |
| Fibrinogen_aC | DP00233 | | 1 |
| Fibrinogen_C | DP00233 | | 1 |
| Flavi_capsid | DP00673 | | 1 |
| Flavi_DEAD | DP00673, DP00674, DP00675 | | 3 |
| Flavi_glycop_C | DP00673 | | 1 |
| Flavi_glycoprot | DP00673 | | 1 |
| Flavi_M | DP00673 | | 1 |
| Flavi_NS1 | DP00673 | | 1 |
| Flavi_NS2A | DP00673 | | 1 |
| Flavi_NS2B | DP00673 | | 1 |
| Flavi_NS4A | DP00673 | | 1 |
| Flavi_NS4B | DP00673 | | 1 |
| Flavi_NS5 | DP00673 | | 1 |
| Flavi_propep | DP00673 | | 1 |
| Fn_bind | DP00025, DP00127 | X3, X5 | 2 |
| fn3 | DP00517, DP00666 | X5, X4 | 2 |
| FtsJ | DP00673 | | 1 |
| Furin-like | DP00309 | | 1 |
| FXR1P_C | DP00134 | | 1 |
| Gag_MA | DP00651 | | 1 |
| Gag_p12 | DP00651 | | 1 |
| Gag_p30 | DP00651 | | 1 |
| GAGA | DP00328 | | 1 |
| Gp5_C | DP00284 | X3 | 1 |
| Gp5_OB | DP00284 | | 1 |
| Gram_pos_anchor | DP00025, DP00121, DP00127 | | 3 |
| HCV_core | DP00674 | | 1 |
| HCV_env | DP00674 | | 1 |
| HCV_NS2 | DP00674 | | 1 |
| HCV_NS4a | DP00674 | | 1 |
| HCV_NS4b | DP00674 | | 1 |
| HCV_NS5a | DP00674 | | 1 |
| HCV_NS5a_1a | DP00674 | | 1 |
| HCV_NS5a_1b | DP00674 | | 1 |
| Helicase_C | DP00560, DP00675 | | 2 |
| Hemagglutinin | DP00566 | | 1 |
| HemolysinCabind | DP00591 | X13 | 1 |
| HLH | DP00224 | | 1 |
| HMA | DP00282 | X6 | 1 |

| | | | |
|--------------------------------|------------------|--------|---|
| Hydrolase | DP00282 | | 1 |
| ILWFO | DP00653 | | 1 |
| RNA_pol_Rpb1_1 | DP00221 | X24 | 1 |
| Involucrin_N | DP00221 | | 1 |
| Ion_trans | DP00228 | X4 | 1 |
| IRS | DP00653 | | 1 |
| I-set | DP00517, DP00666 | X5, X4 | 2 |
| KAT11 | DP00348 | | 1 |
| KH_1 | DP00134 | X2 | 1 |
| KIX | DP00348 | | 1 |
| Kringle | DP00191 | X5 | 1 |
| LRR_1 | DP00554 | | 1 |
| Macscav_rec | DP00246 | | 1 |
| MAP2_projctn | DP00122 | | 1 |
| MNNL | DP00418 | | 1 |
| NACHT | DP00554 | | 1 |
| NIF | DP00177 | | 1 |
| non | DP00441 | | 1 |
| Nuc_rec_co-act | DP00343 | | 1 |
| PAAD_DAPIN | DP00554 | | 1 |
| PAN_1 | DP00191 | | 1 |
| Paramyx_P_V | DP00133 | | 1 |
| PAS | DP00343 | | 1 |
| PD40 | DP00484 | | 1 |
| Peptidase_C28 | DP00573 | | 1 |
| Peptidase_C3 | DP00573 | | 1 |
| Peptidase_C4 | DP00560 | | 1 |
| Peptidase_C53 | DP00675 | | 1 |
| Peptidase_C6 | DP00560 | | 1 |
| Peptidase_C74 | DP00675 | | 1 |
| Peptidase_S29 | DP00674 | | 1 |
| Peptidase_S30 | DP00560 | | 1 |
| Peptidase_S31 | DP00675 | | 1 |
| Peptidase_S41 | DP00484 | | 1 |
| Peptidase_S7 | DP00673 | | 1 |
| Peptidase_S9 | DP00248 | | 1 |
| Phage_Coat_A | DP00034 | | 1 |
| Phage_lysozyme | DP00284 | | 1 |
| PID | DP00154 | | 1 |
| Pkinase_Tyr | DP00309 | | 1 |
| Plug | DP00176 | | 1 |
| Poty_coat | DP00560 | | 1 |
| Poty_PP | DP00560 | | 1 |
| Prion | DP00466 | | 1 |
| Prion_bPrPp | DP00466 | | 1 |
| PTEN_C2 | DP00351 | | 1 |
| RdRP_1 | DP00560, DP00573 | | 2 |
| RdRP_3 | DP00674, DP00675 | | 2 |
| Recep_L_domain | DP00309 | X2 | 1 |
| Rhy | DP00573 | X3 | 1 |
| RNA_helicase | DP00573 | | 1 |

| | | | |
|---------------------------------|------------------|-----|---|
| RNA_pol_Rpb1_2 | DP00181 | | 1 |
| RNA_pol_Rpb1_3 | DP00181 | | 1 |
| RNA_pol_Rpb1_5 | DP00181 | | 1 |
| RNA_pol_Rpb1_6 | DP00181 | | 1 |
| RNA_pol_Rpb1_7 | DP00181 | | 1 |
| RNA_pol_Rpb1_R | DP00181 | X21 | 1 |
| RnaseH | DP00651 | | 1 |
| RRM_1 | DP00324 | X2 | 1 |
| RTX | DP00345, DP00591 | | 2 |
| RTX_C | DP00345 | | 1 |
| rve | DP00651 | | 1 |
| RVP | DP00651 | | 1 |
| RVT_1 | DP00651 | | 1 |
| SAMP | DP00519 | X2 | 1 |
| SdrG_C_C | DP00025, DP00065 | | 2 |
| SH2 | DP00154 | | 1 |
| SRC-1 | DP00343 | | 1 |
| SRCR | DP00246 | | 1 |
| SRF-TF | DP00574 | | 1 |
| Suppressor_APC | DP00519 | | 1 |
| Talin_middle | DP00653 | | 1 |
| TBP-binding | DP00081 | | 1 |
| TNF | DP00460 | | 1 |
| TonB_dep_Rec | DP00176 | | 1 |
| TPP_enzyme_C | DP00398 | | 1 |
| TPP_enzyme_M | DP00398 | | 1 |
| TPP_enzyme_N | DP00398 | | 1 |
| Transketolase_N | DP00427 | X2 | 1 |
| Trypsin | DP00191 | | 1 |
| Tubulin-binding | DP00122 | X4 | 1 |
| VBS | DP00653 | X2 | 1 |
| Vps4_C | DP00435 | | 1 |
| VWA | DP00127 | | 1 |
| VWC | DP00274 | | 1 |
| YSIRK_signal | DP00025, DP00065 | | 2 |
| zf-C2H2 | DP00378 | X2 | 1 |
| zf-TAZ | DP00348, DP00348 | | 2 |
| ZU5 | DP00467 | | 1 |
| ZZ | DP00348 | | 1 |

Table S1: The distribution of 186 Pfam domains composing 65 non-redundant, disordered proteins with significant correlations of Gly. ‘Pfam’ is the Pfam name of a domain. ‘Disprot ID’ is the DisProt 5.1 name of a protein. If more than one protein appear in a cell this represents the fact that a given domain enters more than one protein. ‘Number of domain repeats’ is the number of times that a given domain is repeated in a given protein. ‘Number of proteins’ is the number of proteins that share a given domain.

| | | | | | | | |
|---------|---------|---------|---------|---------|---------|---------|---------|
| DP00570 | DP00472 | DP00386 | DP00317 | DP00238 | DP00152 | DP00076 | DP00003 |
| DP00571 | DP00473 | DP00388 | DP00318 | DP00239 | DP00154 | DP00077 | DP00004 |
| DP00573 | DP00475 | DP00390 | DP00320 | DP00241 | DP00155 | DP00078 | DP00004 |
| DP00574 | DP00482 | DP00392 | DP00321 | DP00242 | DP00156 | DP00081 | DP00005 |
| DP00575 | DP00484 | DP00393 | DP00322 | DP00245 | DP00157 | DP00082 | DP00007 |
| DP00576 | DP00485 | DP00394 | DP00324 | DP00246 | DP00158 | DP00083 | DP00009 |
| DP00578 | DP00486 | DP00395 | DP00325 | DP00247 | DP00159 | DP00084 | DP00011 |
| DP00580 | DP00488 | DP00396 | DP00326 | DP00248 | DP00160 | DP00086 | DP00012 |
| DP00581 | DP00489 | DP00397 | DP00327 | DP00252 | DP00162 | DP00087 | DP00013 |
| DP00582 | DP00490 | DP00398 | DP00328 | DP00253 | DP00163 | DP00088 | DP00014 |
| DP00583 | DP00491 | DP00399 | DP00329 | DP00255 | DP00165 | DP00089 | DP00015 |
| DP00587 | DP00499 | DP00400 | DP00330 | DP00256 | DP00171 | DP00090 | DP00016 |
| DP00591 | DP00500 | DP00401 | DP00332 | DP00257 | DP00172 | DP00091 | DP00017 |
| DP00592 | DP00502 | DP00407 | DP00333 | DP00259 | DP00173 | DP00092 | DP00020 |
| DP00607 | DP00504 | DP00412 | DP00334 | DP00261 | DP00176 | DP00094 | DP00021 |
| DP00608 | DP00505 | DP00415 | DP00336 | DP00262 | DP00177 | DP00095 | DP00025 |
| DP00610 | DP00506 | DP00418 | DP00337 | DP00263 | DP00181 | DP00096 | DP00026 |
| DP00613 | DP00509 | DP00419 | DP00339 | DP00267 | DP00182 | DP00098 | DP00027 |
| DP00616 | DP00510 | DP00422 | DP00341 | DP00268 | DP00184 | DP00099 | DP00028 |
| DP00620 | DP00511 | DP00424 | DP00342 | DP00269 | DP00188 | DP00100 | DP00029 |
| DP00621 | DP00513 | DP00426 | DP00343 | DP00270 | DP00189 | DP00102 | DP00030 |
| DP00623 | DP00514 | DP00427 | DP00344 | DP00271 | DP00190 | DP00103 | DP00031 |
| DP00643 | DP00515 | DP00429 | DP00345 | DP00272 | DP00191 | DP00104 | DP00032 |
| DP00646 | DP00516 | DP00430 | DP00346 | DP00273 | DP00192 | DP00105 | DP00033 |
| DP00651 | DP00517 | DP00433 | DP00347 | DP00274 | DP00193 | DP00106 | DP00034 |
| DP00651 | DP00519 | DP00434 | DP00348 | DP00275 | DP00194 | DP00107 | DP00036 |
| DP00653 | DP00520 | DP00435 | DP00349 | DP00276 | DP00196 | DP00108 | DP00037 |
| DP00655 | DP00521 | DP00436 | DP00350 | DP00279 | DP00197 | DP00110 | DP00040 |
| DP00662 | DP00527 | DP00437 | DP00351 | DP00280 | DP00198 | DP00111 | DP00041 |
| DP00664 | DP00529 | DP00438 | DP00352 | DP00282 | DP00201 | DP00114 | DP00042 |
| DP00666 | DP00530 | DP00441 | DP00353 | DP00284 | DP00202 | DP00117 | DP00043 |
| DP00672 | DP00535 | DP00443 | DP00354 | DP00286 | DP00203 | DP00120 | DP00044 |
| DP00673 | DP00537 | DP00444 | DP00356 | DP00287 | DP00206 | DP00121 | DP00045 |
| DP00673 | DP00538 | DP00446 | DP00357 | DP00288 | DP00207 | DP00122 | DP00046 |
| DP00674 | DP00539 | DP00447 | DP00358 | DP00289 | DP00210 | DP00123 | DP00047 |
| DP00674 | DP00540 | DP00448 | DP00359 | DP00290 | DP00211 | DP00126 | DP00049 |
| DP00675 | DP00541 | DP00449 | DP00360 | DP00295 | DP00214 | DP00127 | DP00051 |
| DP00675 | DP00542 | DP00450 | DP00361 | DP00299 | DP00216 | DP00128 | DP00052 |
| DP00678 | DP00546 | DP00455 | DP00363 | DP00300 | DP00217 | DP00129 | DP00053 |
| DP00680 | DP00554 | DP00457 | DP00365 | DP00302 | DP00218 | DP00130 | DP00054 |
| DP00681 | DP00556 | DP00458 | DP00367 | DP00303 | DP00219 | DP00131 | DP00055 |
| DP00682 | DP00557 | DP00459 | DP00373 | DP00304 | DP00220 | DP00132 | DP00057 |
| DP00683 | DP00558 | DP00460 | DP00374 | DP00305 | DP00221 | DP00133 | DP00058 |
| DP00686 | DP00559 | DP00461 | DP00375 | DP00306 | DP00222 | DP00134 | DP00060 |
| DP00687 | DP00560 | DP00463 | DP00376 | DP00307 | DP00223 | DP00137 | DP00061 |
| DP00690 | DP00561 | DP00464 | DP00377 | DP00308 | DP00224 | DP00138 | DP00062 |
| | DP00562 | DP00465 | DP00378 | DP00309 | DP00225 | DP00141 | DP00063 |
| | DP00563 | DP00466 | DP00379 | DP00310 | DP00228 | DP00143 | DP00064 |
| | DP00564 | DP00467 | DP00380 | DP00311 | DP00229 | DP00144 | DP00065 |
| | DP00566 | DP00468 | DP00381 | DP00312 | DP00231 | DP00146 | DP00068 |
| | DP00567 | DP00469 | DP00382 | DP00313 | DP00232 | DP00147 | DP00069 |
| | DP00568 | DP00470 | DP00383 | DP00314 | DP00233 | DP00148 | DP00071 |
| | DP00569 | DP00471 | DP00385 | DP00315 | DP00235 | DP00151 | DP00075 |

Table S2: List of disordered proteins used in the correlation analysis.

Human hubs:

| | | | | | |
|------------|------------|------------|------------|------------|------------|
| BC006201.2 | BC032718.1 | BC018396.1 | BC017352.2 | BC031559.1 | BC016902.1 |
| BC022510.1 | BC015356.1 | BC002334.2 | BC001965.2 | BC027478.1 | BC025689.1 |
| BC013796.1 | BC008424.1 | BC008794.2 | BC007770.2 | BC016979.1 | BC030598.2 |
| BC014844.1 | BC005165.2 | BC010146.2 | BC003024.1 | BC008781.2 | BC001966.1 |
| BC032459.1 | BC032410.1 | BC015893.2 | BC004819.1 | BC021721.2 | BC004180.2 |
| BC004817.1 | BC028985.1 | BC011794.2 | BC000966.2 | BC009108.1 | BC027910.1 |
| BC001351.2 | BC000427.2 | BC018121.1 | BC006550.2 | BC017206.2 | BC008284.1 |
| BC013596.1 | BC000163.2 | BC014791.2 | BC024000.1 | BC026311.1 | BC021719.2 |
| BC000995.2 | BC026902.1 | BC008950.2 | BC012443.1 | BC036016.1 | BC022983.1 |
| BC003394.1 | BC026092.1 | BC032606.2 | BC039294.1 | BC002607.2 | BC012332.1 |
| BC000355.2 | BC000103.2 | BC020970.1 | BC010456.1 | BC017091.1 | BC018555.1 |
| BC002641.2 | BC015935.1 | BC008796.2 | BC010889.1 | BC003183.1 | BC015239.1 |
| BC007628.1 | BC003565.1 | BC003608.2 | BC036022.1 | BC007654.2 | BC031090.1 |
| BC002448.2 | BC015030.1 | BC000714.2 | BC007780.2 | BC001080.2 | BC035763.1 |
| BC004479.2 | BC001093.2 | BC010561.1 | BC000244.1 | BC012945.1 | BC018070.1 |
| BC007836.2 | BC000404.2 | BC008740.2 | BC011454.1 | BC011806.2 | BC014590.2 |
| BC036012.1 | BC029836.1 | BC036380.2 | BC022536.1 | BC031038.1 | BC034422.1 |
| | BC020090.1 | BC003104.1 | BC005197.1 | BC015708.2 | BC002899.1 |

Human orphans:

| | | | | |
|------------|------------|------------|------------|------------|
| BC015878.1 | BC026340.1 | BC001619.1 | BC008145.1 | BC008397.1 |
| BC010530.1 | BC013780.1 | BC009245.1 | BC008718.2 | BC016481.1 |
| BC032309.1 | BC025722.1 | BC013584.2 | BC012889.1 | BC017251.2 |
| BC008990.1 | BC029831.1 | BC007685.2 | BC004371.1 | BC002651.2 |
| BC006323.2 | BC037963.1 | BC002430.2 | BC005380.1 | BC008723.2 |
| BC034488.2 | BC036797.1 | BC000260.1 | BC005282.1 | BC006322.2 |
| BC014093.2 | BC000253.1 | BC018538.1 | BC009698.2 | BC015566.2 |
| BC011977.1 | BC012356.1 | BC008813.2 | BC005348.2 | BC031609.1 |
| BC039063.1 | BC014214.2 | BC035217.1 | BC027977.1 | BC000006.2 |
| BC005377.1 | BC036283.1 | BC009647.1 | BC007402.2 | BC011835.2 |
| BC013756.1 | BC021245.2 | BC007711.2 | BC004369.1 | BC005302.1 |
| BC010942.1 | BC027881.1 | BC034376.1 | BC005307.1 | BC035588.1 |
| BC006195.2 | BC012392.1 | BC007060.1 | BC012479.1 | BC029059.1 |
| BC010425.1 | BC022447.1 | BC008664.1 | BC013566.1 | BC019310.1 |
| BC008493.1 | BC032688.1 | BC001275.1 | BC009799.1 | BC016512.1 |
| BC014588.2 | BC011564.1 | BC009564.1 | BC011358.1 | BC000931.3 |
| BC012597.1 | BC011606.2 | BC000182.1 | BC000043.2 | BC002389.2 |
| BC033867.1 | BC009474.1 | BC004993.1 | BC008918.2 | BC005366.1 |
| BC000254.1 | BC001116.2 | BC017046.1 | BC029050.1 | BC004963.2 |
| BC035568.1 | BC016180.1 | BC002632.2 | BC012513.1 | BC030640.2 |
| BC012290.1 | BC000479.2 | BC025698.1 | BC016031.1 | BC013393.2 |
| BC007678.2 | BC011798.2 | BC004926.2 | BC014261.2 | BC005127.2 |
| BC004370.1 | BC030230.2 | BC010854.2 | BC007000.1 | BC014665.1 |
| BC007058.1 | BC002967.1 | BC027946.1 | BC007427.2 | BC014210.2 |

Table S3: List of human hubs and orphans used in the correlation analysis.

| | | | | | | | | | |
|--------|-------|--------|---------|---------|--------|--------|--------|--------|--------|
| SSA1 | ENP1 | ARO1 | UTP7 | GCN1 | SPO12 | RSC4 | TAF11 | RIO2 | ISW2 |
| TPD3 | MRPS5 | HPR1 | PUP3 | YIP4 | PRP8 | GCN3 | YML6 | SSU72 | SNU66 |
| CCR4 | SRB6 | TAF12 | RAD51 | CHC1 | CDC23 | NAP1 | VPS71 | CSL4 | NOP58 |
| MYO4 | TRS20 | TAF10 | KAP123 | SPT16 | UTP9 | BET3 | PRP39 | SIN4 | MYO2 |
| PRP45 | HSM3 | SEC7 | LSM4 | DOC1 | RIX1 | RPF2 | RSE1 | SUI1 | VMA4 |
| MTW1 | PAF1 | SUP35 | RSP5 | SWC4 | RPN10 | SPA2 | TEM1 | POL2 | RPA190 |
| FUN12 | SNF5 | NGG1 | NSA2 | TFG2 | BET1 | PRP19 | ORC1 | YIF1 | PRT1 |
| CDC24 | SGF29 | RVB1 | GLC7 | SEC9 | RPB3 | SED5 | POB3 | IST1 | PRE10 |
| PTA1 | GBP2 | NUP42 | LSM5 | SNU71 | CKA1 | RSC58 | PRE8 | BNI1 | TAF3 |
| NUP60 | KRR1 | REF2 | SPT15 | VMA7 | NOT3 | PDC1 | TAF13 | MRPL10 | RRP12 |
| RFA1 | HTL1 | GCD6 | BEM2 | KSS1 | SNP1 | SPT8 | TAF8 | SEC21 | SWI1 |
| HTB2 | RRP43 | SIR4 | COG3 | TFC4 | RPN2 | RGR1 | RSC9 | PFS2 | CTF19 |
| HTA2 | TAF2 | PCF11 | CHD1 | RSC1 | LYS12 | BUD20 | TAF4 | RPD3 | PHO85 |
| UTP20 | RSC6 | PRP42 | PAB1 | SMD1 | SEC24 | SIC1 | ARP9 | RPC34 | SSN3 |
| SLA1 | PWP2 | SEC26 | RAD3 | UTP22 | NUP159 | CDC45 | NUP116 | CSE2 | NOP4 |
| FUS3 | PAT1 | SNU56 | BRR2 | PRP31 | STH1 | MDN1 | ERB1 | TIM23 | SGF11 |
| MCM2 | TUP1 | SWM1 | DMC1 | DBF2 | PAN1 | HOG1 | RNA14 | MRPS12 | MOT1 |
| LSM2 | ABP1 | RRP45 | IES1 | RRP46 | MND2 | CFT2 | CTF18 | POP2 | NOG1 |
| HEK2 | CDC39 | GCN2 | SMX2 | NOP7 | PRE3 | CLF1 | NAM7 | NOG2 | NAN1 |
| POL12 | NHP10 | CFT1 | EPL1 | SRB5 | OST1 | APC2 | NPL6 | SIN3 | TAF14 |
| MRPL16 | MED2 | RSC3 | YPT1 | DAM1 | RPC17 | DIP2 | UTP15 | HTZ1 | UME1 |
| URA7 | RPT2 | SRB7 | ACT1 | NUP57 | HCA4 | SMD3 | MYO5 | DIS3 | PRP46 |
| SEC17 | APC11 | TFB1 | LOC1 | COG2 | NSP1 | CBF5 | ASC1 | PRE6 | RAD53 |
| CDC27 | NOP1 | MCM21 | RPN11 | UTP8 | UTP18 | RFX1 | SPC24 | GAL11 | CBC2 |
| RPL23A | ARP2 | UTP4 | UBP6 | CBF2 | ARP4 | SAM1 | STO1 | BRX1 | CTI6 |
| ROX3 | PRP9 | SKP1 | LSB3 | PTI1 | UTP10 | EMG1 | ECM16 | MSH2 | HRR25 |
| ATP1 | DBP10 | SWR1 | ECO1 | MTR3 | ASF1 | PWP1 | TIF34 | HRP1 | NIP7 |
| PKC1 | SIR2 | SPC110 | CDC14 | TIF4631 | LSM1 | NOP56 | VTI1 | MED7 | LEA1 |
| HHF1 | PRP11 | EAF1 | RPL2A | YIP1 | RPB4 | SEC13 | CEF1 | CDC33 | BMS1 |
| HHT1 | SIT4 | SEM1 | PHO4 | OKP1 | FAR1 | UTP13 | UBP8 | RRP40 | RVB2 |
| KAP104 | LHP1 | LSM6 | CDC26 | TFG1 | SWI3 | CDC42 | TAF7 | CTR9 | SUI3 |
| PRP6 | TSR1 | YRA1 | RSC8 | SKI6 | CDC6 | YEF3 | RRP5 | SPT20 | HSP82 |
| ORC2 | RXT3 | RVS167 | PRE4 | ELP2 | PRP21 | YPT6 | TAF9 | DCP1 | GAL4 |
| RPG1 | SUB2 | SPT3 | RET2 | CRM1 | MPP10 | SEC22 | CUS1 | RRP6 | HFI1 |
| SPT7 | LUC7 | RPT3 | RPN12 | MRPL9 | SUI2 | SMD2 | ZDS1 | PEP12 | CLN2 |
| MIS1 | RPN6 | SXM1 | CDH1 | NAS6 | LSM8 | YSH1 | HSH155 | CKB2 | RPA135 |
| RFC5 | RRP42 | RPB7 | SCL1 | PFK1 | RPA12 | GCD7 | HAS1 | CKA2 | TIF6 |
| POL30 | NUP84 | SYF1 | CKB1 | SDA1 | CDC11 | GSP1 | PSE1 | RPL3 | EAF3 |
| NHP6B | CDC48 | RPN9 | PGD1 | GCN5 | FIP1 | YHC1 | NIP1 | SKI7 | ARP7 |
| EXO84 | CDC53 | TIF35 | RPT6 | TAF1 | RSM7 | CDC25 | PRE5 | BUD21 | TIF5 |
| SIF2 | RPO21 | NPL3 | TIF4632 | RTT102 | ATP2 | CDC3 | RLP7 | NUP1 | MCM16 |
| CMD1 | COP1 | SSN2 | DUO1 | MRP4 | RPS4A | BUD6 | LST8 | VAM3 | MED1 |
| CYC8 | RPN5 | ADA2 | SGF73 | SNF6 | PRP40 | SFH1 | PUB1 | RPO31 | NOT5 |
| RAD16 | NOP14 | UTP6 | RPB9 | ECM29 | URB1 | NUP2 | SSN8 | RPT5 | SUA7 |
| MUD1 | RPC53 | TLG1 | NUP145 | SBP1 | SWD2 | FKS1 | YIP3 | RPB2 | SNT309 |
| TPS1 | DHH1 | PRP3 | LSG1 | YSC84 | CDC16 | KAP95 | NOP2 | SME1 | PRE2 |
| VMA2 | TFP1 | SNF1 | NSA1 | RPN1 | NUP120 | RSC2 | TOP2 | MED4 | YTH1 |
| CKS1 | SEC31 | PUF6 | TAF6 | SLT2 | MPE1 | STE11 | POL1 | LAS17 | RPN7 |
| MAK5 | NHP2 | SMT3 | SNF4 | SRB2 | NUP100 | IKI3 | YAF9 | NOC2 | RPC40 |
| SUP45 | CWC2 | WBP1 | CDC20 | CIC1 | TEF4 | UTP21 | NOP15 | RPB10 | CLB2 |
| SPP381 | EHD3 | GCN4 | PRP43 | MED6 | YJU2 | CDC73 | RPC19 | STE4 | RRP9 |
| RPB5 | BAP3 | RAD23 | SOH1 | SSF1 | MYO3 | RPN13 | FAR11 | RPB8 | NOC4 |
| CDC28 | MAK21 | NUG1 | CEG1 | RRP4 | RPC25 | ATG17 | KRE33 | ESA1 | RHO1 |
| MED8 | LCB2 | PRE1 | SEC27 | NAM8 | RPT1 | SPP382 | THO2 | APC5 | NUT2 |
| TAF5 | MSH6 | RPN3 | INO80 | RPF1 | RSM22 | LSM3 | LSM7 | RPT4 | PRP4 |
| BEM1 | BMH2 | SRB4 | NUT1 | GAR1 | SNU114 | SIR3 | APC1 | RPN8 | SEC23 |
| PDB1 | ARX1 | GCD11 | NUP49 | YNG2 | YKT6 | SST2 | NOP13 | VPH1 | SMX3 |
| SWC5 | STE5 | SMB1 | KEM1 | TRA1 | VPS1 | YAP1 | SRP1 | YTM1 | RPO26 |
| ISW1 | APC4 | ARB1 | CDC55 | GGA2 | PAP1 | SPT5 | PSY2 | SNF2 | RPC82 |

Table S4: A. List of yeast hubs used in the correlation analysis.

| | | | | | | | |
|-----------|-----------|-----------|-----------|-----------|-----------|-----------|-----------|
| FUN14 | YEL1 | BAP2 | COS111 | YCL012C | THR4 | NDE2 | PHO13 |
| NTG1 | KIP1 | ALG14 | YBR204C | LEU2 | CTR86 | YDL086W | YDL237W |
| YAL018C | SEF1 | YBR071W | ERV15 | YCL021W-A | YCR061W | PMT5 | GUD1 |
| FUN26 | AST1 | YBR072C-A | NGR1 | AGP1 | ATG15 | QRI1 | YDL241W |
| YAL037C-A | YBL071C-B | HSP26 | SDS24 | FRM2 | CPR4 | QRI7 | AAD4 |
| YAL037W | YBL081W | YBR074W | HPC2 | HBN1 | SOL2 | MSS2 | THI13 |
| CYC3 | ALG3 | ECM8 | PYC2 | YCL033C | ERS1 | YDL109C | HXT15 |
| GCV3 | YBL086C | ECM33 | YBR219C | GRX1 | YCR075W-A | YDL114W | SOR2 |
| YAL044W-A | AVT5 | YBR085C-A | YBR220C | GFD2 | YCR076C | YDL118W | MPH2 |
| YAL046C | MAP2 | AAC3 | YBR221W-A | ATG22 | TRX3 | YDL119C | COS7 |
| GEM1 | SCS22 | YBR090C | PCS60 | YCL042W | FIG2 | YDL121C | RCR2 |
| YAL049C | RPL32 | YBR096W | TDP1 | MGR1 | YCR090C | SNA4 | YDR003W-A |
| ACS1 | YBL095W | YMC2 | MCX1 | YCL045C | KIN82 | YDL124W | SOK1 |
| CNE1 | BNA4 | PHO88 | OM14 | YCL047C | CDC50 | VCX1 | TRP1 |
| BDH1 | YBL100W-A | ALG1 | YBR230W-A | SPS22 | YCR095W-A | YDL129W | SNQ2 |
| YAL063C-A | YBL100W-B | YSA1 | YBR235W | YCL048W-A | HMRA2 | STF1 | RPL4B |
| YAL064C-A | YBL100W-C | CBP6 | PRP5 | YCL049C | GIT1 | LYS21 | RAD61 |
| YAL064W | ECM21 | GRS1 | YBR241C | APA1 | YCR100C | RPL41B | HED1 |
| YAL064W-B | SFT2 | OPY1 | YBR242W | KAR4 | YCR101C | YDL133W | YDR018C |
| YAL065C | YBL107C | AGP2 | ALG7 | YCL057C-A | YCR102C | RPL35B | GCV1 |
| SEO1 | YBL108C-A | YBR139W | GPX2 | PRD1 | PAU3 | RGT2 | RAD28 |
| YAL067W-A | YBL111C | YBR141C | YBR246W | YCL058W-A | ADH7 | SCM3 | MIC14 |
| YAR009C | YBL112C | ADH5 | HIS7 | CHA1 | RDS1 | BPL1 | MRH1 |
| KIN3 | YBL113C | RTC2 | ARO4 | YCL068C | AAD3 | YDL144C | LYS14 |
| PAU7 | RER2 | YSW1 | SPO23 | VBA3 | YCR108C | YDL159W-A | YDR034C-A |
| YAR023C | GPI18 | ARA1 | DUT1 | YCL073C | RMD1 | YDL160C-A | YDR034W-B |
| YAR028W | RCR1 | TBS1 | YBR255C-A | MRPL32 | YDL007C-A | CDC9 | ARO3 |
| YAR029W | UGA2 | APD1 | MTC4 | CIT2 | GRX6 | SFA1 | ENA5 |
| PRM9 | DSF2 | RIB7 | RIB5 | YCR007C | YDL012C | UGX2 | YDR042C |
| YAR035C-A | FLR1 | ICS2 | YBR259W | SAT4 | GPM2 | UGA3 | HEM12 |
| YAT1 | YBR013C | YBR159W | TAE1 | ADY2 | GPD1 | YDL173W | DET1 |
| FLO1 | GRX7 | CSH1 | YBR262C | ADP1 | DIA3 | DLD1 | PST1 |
| YAR066W | MNN2 | YSY6 | MRPL37 | YCR016W | YDL027C | YDL176W | YDR056C |
| YAR068W | YBR016W | DEM1 | FMP21 | CWH43 | SLM3 | YDL177C | YOS9 |
| PHO11 | GAL7 | UBS1 | YBR271W | SRD1 | PUS9 | INH1 | TGL2 |
| ECM15 | GAL10 | TYR1 | PPS1 | MAK32 | BSC1 | YDL183C | UBC5 |
| LDB7 | FUR4 | SMY2 | SSH1 | PET18 | PRM7 | NUS1 | YDR061W |
| YBL008W-A | POA1 | ECM31 | YBR284W | HSP30 | FAD1 | ASF2 | YDR063W |
| ALK2 | ETR1 | EHT1 | YBR285W | YCR023C | NPC2 | GGC1 | YDR065W |
| SCT1 | YBR028C | DTR1 | APE3 | SLM5 | STP4 | MGT1 | RTR2 |
| ACH1 | RKM3 | RPS6B | CTP1 | YCR024C-B | KNH1 | MRPL11 | OCA6 |
| RFT1 | EDS1 | YBR182C-A | VBA2 | NPP1 | SLC1 | RTN2 | DOS2 |
| RPL19B | PDX3 | YPC1 | SUL1 | RHB1 | PBP4 | HEM3 | FMP16 |
| YBL028C | CSG2 | YBR184W | PHO89 | FEN2 | MCH1 | YDL206W | IPT1 |
| YBL029C-A | FIG1 | MBA1 | YBR296C-A | RIM1 | YDL057W | UGA4 | PET100 |
| YBL029W | CST26 | PCH2 | MAL33 | BPH1 | RPS29B | YDL211C | PDC2 |
| RIB1 | QDR3 | GDT1 | MAL31 | FEN1 | YDL063C | PRR2 | RRP8 |
| STU1 | ZTA1 | RPL21A | YBR298C-A | RBK1 | CBS1 | GDH2 | YDR089W |
| YBL036C | FMP23 | RIM2 | MAL32 | PHO87 | YET3 | YDL218W | YDR090C |
| YBL039W-B | YBR053C | YBR196C-A | RER1 | MATALPHA1 | YDL073W | FMP45 | GIS1 |
| FUI1 | YRO2 | YBR196C-B | YCL001W-A | PER1 | RPL31A | HBT1 | TMS1 |
| ECM13 | YBR056W | YBR197C | YCL001W-B | YCR045C | MDH3 | WHI4 | ARP10 |
| TOD6 | TSC3 | KTR4 | YCL002C | BUD23 | MRK1 | PTP1 | TMN2 |
| YBL055C | YBR062C | YBR200W-A | PGS1 | ARE1 | RPL13A | BRE4 | YDR109C |
| PTH2 | YBR063C | YBR201C-A | LDB16 | YCR050C | RPS16B | YDL233W | ALT2 |
| YBL059C-A | TIP1 | DER1 | VMA9 | YCR051W | YDL085C-A | GYP7 | YDR114C |

| | | | | | | | |
|-----------|-----------|-----------|---------|-----------|-----------|-----------|------------|
| VBA4 | DPP1 | ERD1 | YDR532C | MIG3 | YER138W-A | YFH7 | ALG2 |
| YDR119W-A | YDR286C | RAD30 | FIT1 | CHZ1 | YER140W | YFR012W | NPY1 |
| TRM1 | INM2 | HKR1 | STL1 | YER034W | COX15 | YFR012W-A | RPL7A |
| KIN1 | HRQ1 | ARO80 | PAD1 | EDC2 | MAG1 | YFR016C | HNMI |
| YDR124W | DPL1 | BNA7 | YDR539W | PHM8 | FTR1 | YFR018C | FMP37 |
| ECM18 | SUR2 | GPI17 | IRC4 | HVG1 | YER152C | PES4 | YGL081W |
| SWF1 | GPI11 | PPM1 | YDR541C | YER039C-A | YER156C | HIS2 | YGL082W |
| MTC5 | CPR5 | GPI19 | YRF1-1 | MXR1 | YER163C | ULI1 | SCY1 |
| SAN1 | HNT2 | THI74 | IRC22 | MEI4 | DNF1 | PTR3 | GUP1 |
| MKC7 | YDR307W | YDR444W | YEA4 | ACA1 | RPH1 | YFR032C | YGL085W |
| EKI1 | SSF2 | YHP1 | YEA6 | SPO73 | ADK2 | RPL29 | MF(ALPHA)2 |
| CTH1 | IPK1 | PPN1 | YEL007W | CAJ1 | TMT1 | YFR032C-B | YGL101W |
| HOM2 | OMS1 | TSA2 | GLC3 | JHD1 | YER175W-A | QCR6 | RPL28 |
| SSY1 | HIM1 | GUK1 | NPP2 | PIC2 | ECM32 | YFR035C | VPS73 |
| CWC15 | ASP1 | HEH2 | PMP2 | YER053C-A | ISC10 | IRC5 | RMD9 |
| YDR169C-A | YSP2 | PFA5 | GTT3 | HIS1 | FMP10 | YFR039C | YGL108C |
| UBC1 | GPI8 | YDR461C-A | YEL020C | FCY2 | FAU1 | ERJ5 | CUE3 |
| SDH4 | IRC3 | MFA1 | URA3 | RPL34A | YER184C | KEG1 | YGL114W |
| YDR179W-A | YDR333C | STP1 | YEL023C | HMF1 | PUG1 | IRC6 | YGL117W |
| CDC1 | YDR336W | RMT2 | YEL025C | PET117 | YER186C | YFR045W | ABC1 |
| YDR182W-A | YDR338C | PKH3 | BUD16 | FCY21 | YER187W | BNA6 | GPG1 |
| PLP1 | FCF1 | RPL27B | MTC7 | CEM1 | YER188C-A | RMD8 | RPS2 |
| YDR185C | YDR341C | JIP4 | UTR5 | THO1 | YER190C-B | HXK1 | SCS3 |
| HST4 | HXT7 | YDR476C | UTR4 | YER064C | DEG1 | IRC7 | MRM2 |
| MSS116 | SVF1 | PHO8 | CYC7 | YER066W | VTC2 | YFR057W | YGL138C |
| YDR194W-A | YPS7 | CWC21 | UTR2 | YER067W | BLM10 | ERP6 | FLC3 |
| CBS2 | SBE2 | KRE2 | GDA1 | ARG5,6 | WWM1 | PMC1 | YGL140C |
| RKM2 | YDR352W | RIB3 | IES6 | VTC1 | YFL012W | YGL006W-A | HUL5 |
| EBS1 | TRP4 | YDR493W | YEL047C | ALD5 | HSP12 | YGL007C-A | MRF1 |
| MSS4 | YDR357C | RSM28 | YEL048C | YOS1 | GAT1 | PMA1 | YGL146C |
| YDR210W | ESC2 | VPS3 | AFG1 | YER076C | BST1 | LEU1 | RPL9A |
| MFB1 | YDR366C | ITR1 | YEL057C | YER077C | GYP8 | YGL010W | ARO2 |
| YDR222W | YDR367W | RPL37B | SOM1 | YER078C | AGX1 | ERG4 | YGL159W |
| ADK1 | YPR1 | LPP1 | CIN8 | YER078W-A | HAC1 | PUF4 | YGL160W |
| HEM1 | YDR370C | SPG3 | NPR2 | YER079W | RPL22B | ATE1 | CUP2 |
| LYS4 | CTS2 | PSP1 | CAN1 | AIM9 | YFL034W | JAC1 | PMR1 |
| FMN1 | VPS74 | YDR506C | AVT2 | YER085C | YFL040W | ALK1 | HUR1 |
| AMD2 | YDR374C | GNP1 | HPA3 | YER087W | YFL041W-A | PIB2 | SUA5 |
| YDR246W-A | YDR374W-A | ACN9 | YEL067C | MET6 | YFL042C | CWH41 | SPO74 |
| YDR248C | BCS1 | EMI1 | DSF1 | YER093C-A | FMP32 | SCW11 | SAE2 |
| YDR249C | ARH1 | GRX2 | DLD3 | SHC1 | RGD2 | CGR1 | YGL176C |
| PAM1 | YDR379C-A | YDR514C | RMD6 | UBP9 | ALR2 | RPL24A | TOS3 |
| RMD5 | ARO10 | SLF1 | YEL073C | AST2 | YFL051C | AGA2 | STR3 |
| CTA1 | YDR381C-A | EUG1 | YEL075C | RTT105 | YFL052W | PNC1 | YGL185C |
| RKM4 | ATO3 | FPR2 | YEL076C | NUP157 | DAK2 | OCH1 | TPN1 |
| HSP78 | YDR387C | URC2 | YEL077C | MAM1 | YFL054C | YGL039W | YGL188C-A |
| EXG2 | YDR391C | SPS2 | MNN1 | FLO8 | AGP3 | HEM2 | COX13 |
| YDR262W | SHE9 | SPS1 | PMI40 | TMN3 | AAD6 | YGL041C-B | IME4 |
| DIN7 | HPT1 | AGE1 | FMP52 | SPR6 | AAD16 | YGL041W-A | YGL193C |
| YDR266C | URH1 | YDR524C-B | YER010C | AVT6 | SNO3 | RIM8 | YGL194C-A |
| MSW1 | DIT2 | YDR524W-C | BUD25 | YER121W | DDI2 | ALG13 | DSD1 |
| | DIT1 | SNA2 | HEM14 | YCK3 | YFL064C | TYW3 | GLO2 |
| | PDR15 | RBA50 | FAA2 | YER128W | YFL065C | ERV14 | BSC2 |
| | ADE8 | HLR1 | ISC1 | YER130C | YFL066C | OLE1 | PMP3 |
| | STE14 | APA2 | YAT2 | YER134C | YFL067W | SDS23 | PHM6 |
| | DFM1 | YDR531W | CHO1 | YER137C | SAD1 | PKP2 | YDR282C |

Table S4: B. List of yeast orphans used in the correlation analysis.

| | | | | | | | | | | |
|------|------|------|------|------|------|------|------|------|------|------|
| aidB | rpoZ | pgk | otsA | dps | talB | rplB | gltD | yfdH | treA | metN |
| ulaR | rpmB | metK | uvrC | yliG | dnaJ | rpsS | rpsI | tktB | prsA | gmhB |
| rpsF | rpmG | hybG | yodC | potF | rpsT | rpsC | rplM | yfgB | lolB | rnhA |
| rpsR | rfaD | hybC | dcm | ybjX | fkpB | rplP | yhdP | iscU | kdsA | dnaQ |
| rplI | yibL | exbD | flu | cspD | apaH | rpmC | mreB | srmB | narG | proC |
| Ppa | selB | exbB | yeeX | clpA | murE | rplN | hupA | yfiD | hns | mak |
| yjgA | glyQ | parC | wbbK | pflB | murF | rplX | nfi | yfiF | adhE | tgt |
| yjgF | cspA | parE | wcaI | rpsA | murC | rplE | rpoC | yfiQ | rluB | ribD |
| holC | yhjD | ygiF | yeiT | mukB | ftsZ | rpsN | rpoB | pssA | topA | cyoC |
| fimB | ftsE | rpsU | rplY | fabA | secA | rpsH | rplL | clpB | acnA | tig |
| fimA | ugpB | rpoD | rcsB | ompA | acnB | rplF | rplJ | rplS | yciS | clpP |
| hsdM | yhhX | yqjI | gyrA | helD | yacL | rplR | rplA | rpsP | ycjF | lon |
| hold | malP | yqjD | yfaY | yccW | yadG | rplO | rplK | ffh | hrpA | hupB |
| rimI | mrcA | deaD | elaB | hyaA | pcnB | rpsM | nusG | grpE | ydcP | ybaY |
| yjjU | rpe | pnp | nuoG | cbpA | pyrH | rpsK | tufB | smpB | yncE | dnaX |
| serB | slyD | rpsO | nuoC | putA | yaeT | rpsD | hslU | intA | gadB | ybaS |
| yjeE | rpsL | infB | yfbR | rne | hlpA | rpoA | polA | gabD | ydfG | allR |
| Hfq | fusA | nusA | yfbU | rluC | lpxD | rplQ | dsbA | ygaM | lhr | ybcJ |
| purA | rpsJ | ftsH | pta | acpP | fabZ | yjbH | uvrD | csrA | pykF | ahpC |
| Rnr | rplD | yhbY | argT | holB | dnaE | dnaB | rho | recA | ydiI | uspG |
| dnaN | rplW | rplU | yfcZ | ymfD | accA | ssb | rhlB | hypC | ihfA | cspE |
| gyrB | groL | trmE | nudH | topB | nagB | fdhF | atpA | hypD | rplT | holA |
| ibpA | blc | rnpA | ygfK | ydjL | pgm | yjdJ | atpD | nlpD | infC | leuS |
| spot | rsgA | dnaA | ygfU | gapA | ybgI | groS | pstB | eno | thrS | ybeZ |
| lysS | yoaB | gltA | recJ | kdgR | sucC | gevp | holE | ybgC | yggE | torZ |
| ybhK | | | | | | | | | | |

Table S5: A. List of *E. coli* hubs used in the correlation analysis.

| | | | | | | | | | | | | | |
|------|------|------|------|------|------|------|---------|------|------|------|---------|------|------|
| cusF | ybbA | yaiY | insF | yafN | pdhR | thrL | ybeH | ybcS | hha | mhpB | yagQ | nlpE | thiQ |
| cusB | rhdD | yaiZ | ykgA | yafO | aceE | thrB | ybeM | rzpD | acrR | mhpC | yagR | yaeF | sgrR |
| cusA | ylbH | iraP | ykgB | yafP | aceF | yaaX | tatE | rzoD | ybaM | mhpD | yagS | rscF | setA |
| ybdG | ybbD | psiF | ykgI | prfH | lpd | yaaJ | ybeF | borD | ybaN | mhpT | yagT | metI | leuB |
| nfnB | ybbB | adrA | ykgD | gpt | yacH | yaaH | lipB | ybcW | recR | yaiO | yagU | dkgB | leuL |
| ybdJ | allS | yaiI | ykgE | crl | speE | htgA | rlpA | nohB | hemH | insC | ykgJ | yafE | leuO |
| ybdK | allA | aroL | ykgF | proB | yacC | yaaI | ybeA | ybcY | aes | insD | yagV | yafS | mraY |
| hokE | glxR | aroM | ykgG | ykfI | cueO | dnaK | cobC | ylcE | fsr | tauA | yagW | yafT | ddlB |
| entD | ybbV | yaiE | ykgH | yafW | yadH | insL | nadD | appY | ybaP | tauB | matC | yafU | ftsQ |
| fepA | ybbW | ykiA | betA | ykfH | yadI | mokC | rlpB | ompT | ybaQ | tauC | matB | yafF | secM |
| ybdZ | allB | araJ | betI | ykfG | panD | nhaA | ybeL | envY | copA | tauD | matA | ivy | yacF |
| fepE | ybbY | sbcD | betT | yafX | yadD | nhaR | ybeQ | ybcH | cueR | ykiB | ykgL | fadE | hofC |
| fepC | glxK | acpH | yahA | ykfF | yadK | insB | djlB | nfrB | ybbJ | yaiT | ykgM | yafJ | hofB |
| fepD | allD | secF | yahB | ykfB | yadL | insA | ybeT | cusS | qmcA | yaiU | ykgM_v2 | yafK | ppdD |
| entS | fdrA | yajD | yahC | yafY | yadM | yaaY | ybeU | cusR | ybbM | yaiV | eaeH | yafL | ampD |
| fepB | ylbF | tsx | yahD | ykfA | yadN | caiF | djlC | cusC | tesA | sbmA | insE | dinB | aroP |
| entB | ybcF | yajI | yahE | insN | folK | caiE | citT | sfmF | ybaV | prpC | yagB | pfs | ksgA |
| entA | purK | nrdR | yahG | insI | ligT | caiD | citG | intD | ybaW | prpD | yagE | cdaR | pdxA |
| ybdB | purE | thiL | yahH | insO | fhuA | caiB | citX | ybcC | queC | prpE | yagF | yaeI | imp |
| cstA | cysS | pgpA | yahI | ykfC | fhuC | caiA | citF | ybcL | ybaE | codB | yagH | glnD | djlA |
| ybdD | ybcI | yajL | yahL | insH | fhuD | fixA | citE | ybcM | cof | cynR | yagI | rpsB | yabP |
| ybdM | sfmA | panE | yahM | mmuP | hemL | fixC | citD | ybcN | ybaO | cynS | argF | cdsA | yabQ |
| ybdN | sfmC | yajR | yahN | mmuM | clcA | fixX | citC | ninE | mdlB | cynX | yagK | rseP | polB |
| ybdO | sfmD | ampG | yahO | afuB | yadS | yaaU | citA | ybcO | amtB | lacA | yagL | rnhB | araD |
| rna | sfmH | yajG | prpB | ykgN | btuF | apaG | dcuC | rusA | tesB | lacY | yagM | rof | araA |
| crcB | essD | ylaC | mhpA | yagP | yaeJ | yaeQ | dcuC_v2 | ylcG | ybaA | lacZ | yagN | yaeP | araB |
| crcA | ybcQ | ylaB | lacI | intF | nagD | gltK | rihA | araC | | | | | |

Table S5: B. List of *E. coli* orphans used in the correlation analysis.